A nuclear localisation signal in the herpesvirus protein VP1-2 is essential for infection via capsid routing to the nuclear pore.

Abaitua, F., Hollinshead, M., Bolstad, M., Crump,C.M[1]. and O'Hare P*

Section of Virology, Faculty of Medicine, Imperial College, London, W2 1PG, United Kingdom. [1]Division of Virology, University of Cambridge.

* Corresponding author
Tel: 44 (0)207 594 9517
Email: P.OHare@imperial.ac.uk

Running title: The role of the NLS in Herpes simplex virus VP1-2

ABSTRACT

To initiate infection, herpesviruses must navigate to and transport their genomes across the nuclear pore. VP1-2 is a large structural protein of the virion, conserved in all herpesviridae and plays multiple essential roles in virus replication including in early entry. VP1-2 contains an N-terminal basic motif which functions as an efficient nuclear localisation signal (NLS). Here we construct a mutant HSV strain, K.VP1-2ΔNLS, which contains a short 7 residue deletion of the core NLS at position 475. This mutant fails to spread in normal cells, but can be propagated in complementing cell lines. Electron microscopy (EM) analysis of infection in non-complementing cells demonstrated capsid assembly, cytoplasmic envelopment and the formation of extracellular enveloped virions. Furthermore extracellular virions isolated from non-complementing cells had similar profiles and abundance of structural proteins. Virions containing VP1-2ΔNLS were able to enter and be transported within cells. However further progress of infection was prevented, with at least a 500-1000 fold reduction in the efficiency of initiating gene expression compared to the revertant. Ultrastructural and immunofluorescence analysis reveal that the K.VP1-2ΔNLS mutant was blocked at the microtubule organising centre or immediately upstream of nuclear pore docking and prior to gene expression. These results indicate that the VP1-2 NLS is not required for the known assembly functions of the protein but is a key requirement for early routing to the nuclear pore necessary for successful infection. Given its conservation we propose this motif may also be critical for entry of other classes of herpesviruses.

INTRODUCTION

The nuclear pore is the conduit for transport between the cytoplasm and nucleus and as such represents an obligatory pathway that must be navigated very early after infection by many classes of human viruses (9, 20, 21, 27, 36, 44, 50, 60, 62). For herpesviruses, capsid-tegument assemblies must be transported across the cytoplasm, targeted to and interact with pores, and undergo structural rearrangements promoting genome exit and transport across the pore where virus immediate-early gene transcription ensues (14). A prime candidate within the virus

encoded proteins for a possible role at this stage of infection is the large tegument protein VP1-2, the product of the UL36 gene in herpes simplex virus (HSV). This protein is conserved across the herpesvirus family and essential for virus replication (13, 15, 31, 34, 38). It is a complex, multifunctional protein playing crucial and distinct roles at various points in the virus life cycle including entry, capsid transport and virion assembly (7, 13, 15, 31, 34, 38, 52, 55). Consistent with a role at the earliest stages of infection, VP1-2 is among a subset of components classed as inner tegument proteins based on tight association with capsids during biochemical extraction and in vivo during entry by immunoelectron and confocal microscopy (19, 30, 37, 40, 45, 51, 61). Evidence for a key role for VP1-2 early after infection originated from studies of the temperature sensitive mutant virus tsB7 where at the restrictive temperature, full capsids accumulated at the nuclear pore and virus gene expression was profoundly blocked (5, 31). The defect in tsB7 was mapped specifically to a single amino acid at residue 1453 in VP1-2 (1). Supporting evidence for a role in nuclear entry was obtained from studies of a full deletion mutant of the UL36 gene (52). While this mutant does not assemble virions, the authors examined a potential role for VP1-2 by chemically fusing initially infected cells with surrounding cells and measuring infection in these secondary nuclei. The UL36 deletion mutant was completely unable to infect such nuclei in the fused polykaryocytes while in parallel, a UL36+ve but UL37-ve virus was able to promote infection.

However as indicated above, VP1-2 also clearly plays a pivotal role later in infection in virion assembly. Thus an additional late defect was identified in strains carrying the ts VP1-2, resulting in defective cytoplasmic envelopment and a failure to produce infectious virus (1, 3, 4). Furthermore, analysis of VP1-2 deletion mutants have shown that while C-capsids assemble relatively normally in the nucleus, cytoplasmic envelopment and production of infectious virus is completely blocked (13, 15, 52), indicating a critical role in assembly after capsid formation. Current work indicates that, consistent with its definition as an inner tegument protein, that VP1-2 is among the first proteins, if not the first, to be recruited onto assembled capsids and is essential for the further recruitment of additional tegument proteins and subsequent envelopment (15, 30, 32, 52). VP1-2 has also been reported to have additional functions, including capsid motility on microtubules, a role that could also be connected to assembly (37, 38, 51, 55, 61). The protein also encompasses a unique class of ubiquitin specific protease embedded within its extreme N-terminus

(28, 54) which while potentially dispensable for core functions of virus assembly in tissue culture, may play a role in aspects of replication in vivo (24, 35).

However, the essential nature, the multiplicity of roles and the very large size of VP1-2 has made difficult the mechanistic dissection of pathways in which it is involved. In particular considering the dual roles in assembly and in entry, deletion of the protein results in failure to assemble virions and prevents further analysis of its role in entry. Progress in characterisation of specific determinants and a mechanistic framework with which to understand the detailed mechanisms involved requires identification of variants which support virion assembly but remain defective for replication. Such variants represent candidates for a role in virus entry. As part of our aim to understand both herpesvirus early entry mechanisms and the multiplicity of role(s) of VP1-2, we previously demonstrated that VP1-2 contains an efficient nuclear localization signal (NLS) adjacent to the N-terminal ubiquitin hydrolase domain. A similar motif in the PRV VP1-2 homologue has also been shown to be functional in nuclear localisation (43). Here we construct and analyse a HSV mutant containing a short deletion of this NLS. Our data indicate that the short NLS at position 475 in VP1-2, which exhibits strong positional and sequence conservation in the homologues in all herpesviruses (2), is essential for virus spread and further that while dispensable for virion assembly per se, it is key to normal entry early in infection via routing to the nuclear pore.

MATERIALS AND METHODS

Cells, virus, infections and transfection.

Vero and HS30 cells, a derivative of Vero cells containing the UL36 gene (13), were grown in Dulbecco's modified minimal essential medium (DMEM, Gibco) containing 10% newborn calf serum (NCS) and penicillin/streptomycin. RSC (rabbit skin cells) and RSC-HAUL36 cells, a derivative of RSC cells containing the UL36 gene (52) were grown in DMEM containing 10% foetal calf serum (FCS) supplemented with non-essential amino acids. HS30 and RSC-HAUL36 were propagated in 0.5 and 10 mg/ml respectively of geneticin. For some experiments we used HaCaT cells (human keratinocytes) grown in DMEM containing 10% FCS. Not only do these cells represent a relevant cell type for HSV replication, but from comparative analysis we

obtained a several fold increase in extracellular virus yields of any strain analysed, and therefore used these to produce w/t and mutant viruses. Routine characterisation of virus infection was performed exactly as described previously (6).

Construction of a virus mutant expressing VP1-2ΔNLS.

A mutant virus expressing VP1-2 lacking the core NLS was constructed in the background of HSV-1 strain KOS previously cloned in a bacterial artificial chromosome (16). The BACmid was grown in E. coli strain GS1783. The strategy involved recombinational insertion of a cassette for kanamycin resistance adjacent to the mutated sequence, selection for kanamycin resistance, followed by recombination excision and counter selection was carried out exactly as described previously (6). PCR was carried out with the primers below using pEPKan-S (57) as a template. Template DNA was digested by incubating the PCR reaction mix with 20 U DpnI for 1 h at 37°C and the PCR product was purified using a QIAQuick Gel extraction kit (Qiagen) after separation on a 0.8% agarose gel.

COL414: Forward primer for UL36 NLS deletion

CGTCCCGGTTGGTCGGCACCGGGCACGCTACTCGGCCGGCACCTGGACTCCG CCTTC CAGAGGATGACGACGATAAGTAGGG

COL417: Reverse primer for UL36 NLS deletion

CCGAAGTCAGGTCTTCGACGCTGGAAGGCGGAGTCCAGGTGCCGGCCGAGTA GCGTG CCCCAACCAATTAACCAATTCTGATTAG

The PCR product (100 ng) was electroporated and bacteria selected for resistance to chloramphenicol and kanamycin. Resistant colonies were screened by restriction digest. Appropriate colonies were grown and I-SceI induced and the culture heat-shocked at 42°C for 30 min. Candidate colonies that had lost the kanamycin resistance gene were identified by replica plating and BAC DNA isolated and examined by restriction digestion. BAC DNA (100 μg) together with 1 μg pGS403 encoding Cre recombinase, was then transfected into HS30 cells to reconstitute HSV-1 and excise the BAC backbone from the viral genome. Plaques were isolated and multiply plaque-purified in complementing RSC-HAUL36 cells. These cells were used for subsequent routine propagation since spontaneous revertants were not produced while in complementing HS30 cells, revertants were observed, (though still with a low frequency). The mutant virus was designated K.VP1-2ΔNLS. The

presence of the deletion covering 7 residues of the VP1-2 NLS substitution was confirmed by sequencing the first 1353 nucleotides from purified DNA stocks of mutant or parental virus isolates. No other mutations were observed in this region and this fragment was sufficient to rescue K.VP1-2ΔNLS by cotransfection with viral DNA and recombination. A revertant of K.VP1-2ΔNLS was generated by co-transfecting DNA from the K.VP1-2ΔNLS mutant virus together with the w/t UL36 gene, followed by growth and plaque purification on non-complementing RSC cells. The revertant virus was designated K.VP1-2ΔNLS.R. Restoration of the deleted residues was confirmed by sequencing DNA from the isolated revertant virus. For purification of extracellular virions by gradient centrifugation, RSC-HAUL36 cells were infected with K.VP1-2ΔNLS or the revertant at a moi of 0.001 and the medium collected after complete cpe, clarified by centrifugation (2000 rpm 10 min) and virus pelleted from the supernatant by centrifugation at 19k for 90 min. The pellet was then resuspended in PBS (overnight at 4^0C) and loaded onto 5-15% Ficoll gradients made in PBS and samples centrifuged at 25k rpm for 2 h. The lower band containing enveloped virions was extracted by needle puncture, concentrated (25k rpm for 60 min) and the pellet then resuspended in PBS and frozen.

Purification of viral DNA from K.VP1-2ΔNLS.

For purification of viral DNA, RSC-HAUL36 cells (10 x 175 cm^2 flasks) were infected (moi 0.001) and virus isolated from the medium after advanced cpe was observed. The media was first clarified by centrifugation (2k rpm for 20 min) and virus pelleted from the supernatant (19k rpm for 90 min). The pelleted virus was resuspended gently in 5 ml of buffer (10 mM Tris-Hcl [pH 7.6], 1 mM EDTA, 1% SDS), containing 50 μg/ml proteinase K and incubated at 50°C for 4 h and DNA extracted by successive rounds of phenol and phenol/chloroform extraction. The final aqueous phase was precipitated by addition of 0.1 volumes 3M sodium acetate [pH5.3] and 2 volumes of EtOH, gentle mixing and incubation at -20^0C for 30 min. Finally, the DNA was pelleted (3500 rpm for 30 min) at 4°C and washed with 70% EtOH and air dried, then resuspended in 100-200 μl of H_20. The DNA was stored at -80°C.

Immunofluorescence studies.

Immunofluorescence analysis was performed exactly as described previously (3) using the following antibodies: ICP4 (Virusys, 1:400); ICP8 (a kind gift from Roger Everett, 1:2000), pUL37 (a kind gift from Prashant Desai, 1:800); VP16 (LP1 antibody, a kind gift from Tony Minson, 1:400); VP5 (East Coast Bio, 1:500); polyclonal VP1-2, (αVP1-2NT1r, 1:250) (3); monoclonal VP1-2 (CB4, 1:2) and anti PCM1, (Santa Cruz Technologies, 1:50). PCM1 was used for detection of the region around the microtubule organising centre since it gave better staining under conditions for capsid detection than other markers tested, such as γ-tubulin. Samples were collected at times indicated, washed with PBS, fixed with methanol (5 min at -20^{0}C) and blocked with PBSB (PBS containing 10% NCS), supplemented for αVP1-2NT1r with 0.5 mg/ml human IgG (Sigma) for 1 h at room temperature. After processing images were collected using Zeiss x10, x40 LD or x100 (Plan-Apochromat, 1.4 numerical aperture) lenses. Images for each channel were captured sequentially with a Retiga 2000R camera using Image Pro plus software. Composite illustrations were prepared using Adobe software. Example images shown are representative of numerous images gathered for each virus and condition. For studies of the presence and subcellular distribution of HSV virions, infections were performed at a moi of 100. The cells were pre-chilled at 4^{0}C prior to infection. The monolayers were washed once with cold media and the inoculum added for further incubation at 4^{0}C for 1 h. The inoculum was then removed, pre-warmed media containing 2% NCS was added and the cells incubated for different lengths of time at 37^{0}C. The samples were then washed three times with cold PBS and fixed 3.7% PFA in PBS for 20 min at room temperature, and permeabilised with 0.1% TritonX-100 prior the incubation with anti-VP5, pUL37, VP1-2 (CB4) or anti-PCM1 antibody. Controls included parallel analysis of infected cells incubated at 4^{0}C without shifting to 37^{0}C. Images for capsid localisation were collected with a Zeiss LSM510 confocal microscope x40 or x63 Plan-Apochromat, 1.4 numerical aperture lenses. For studies of viral entry, so as not to be selective, images were collected throughout the cell in multiple Z-stacks, compiled and the total images shown. To demonstrate the capsid congregation around the microtubule organising centre (MTOC) e.g., Figure 7, single confocal slices were taken using a pinhole size of 2. Channels were captured sequentially using Axiovision acquisition software and composite illustrations

prepared using Adobe software. For quantitation of capsid localisation, a region of interest (ROI) comprising a 2 μm diameter circle centred around the MTOC (identified by PCM1 staining) was defined for each cell in a field. In an unbiased way, i.e. including all cells with definable MTOCs, these ROIs were then applied to the green channel capsid (VP5 localisation), and the pixel intensity calculated for every ROI after background subtraction. This analysis was performed for approximately 100 cells in several independent fields for the mutant or revertant virus. The results were plotted as the pixel intensity within each MTOC-associated ROI for each cell, for each virus.

Electron microscopy studies.

For analysis of assembly (Figure 5) RSC or Vero cells were infected with KOS w/t or K.VP1-2ΔNLS at a moi of 5 and processed 16 h after infection. For early entry studies (Figure 8,9) cells were infected at a moi of 500. Cells were washed with ice-cold PBS and fixed for 30 min at room temperature in 0.5% glutaraldehyde in 200 mM sodium cacodylate buffer, washed in buffer and processed into Epon and sectioned. Samples were viewed by using an FEI Tecnai G2 electron microscope (FEI, Eindhoven, The Netherlands) with a Soft Imaging System Megaview III charge-coupled device camera. Images were collected at 1,376 × 1,032 × 16 pixels by using analysis version Docu software (Olympus Soft Imaging Solutions, Münster, Germany). For staining of virus particles, suspensions of extracellular pelleted virus were absorbed onto 400 mesh formvar carbon coated glow discharged grids and negatively stained with 1% uranyl acetate.

SDS-PAGE and Western blotting.

Mock or infected cell monolayers were harvested in standard SDS sample buffer. Samples were lysed either using a sonicator waterbath or by needle shearing using a 25G needle and boiled for 5 min prior to electrophoresis. Equal cell samples were analysed on 3-8 % gradient Tris-acetate gels or 10% Tris-glycine gels and transferred to nitrocellulose membranes. Membranes were blocked in PBS containing 0.5x blocking solution (Licor Biosciences). Primary and secondary antibodies for immunodetection were diluted in PBST (PBS plus 0.1% Tween 20 containing 5 % dried milk). Target proteins were visualized using DyLight-conjugated

secondary antibodies (Pierce 1/10000) and developed using Li-Cor Bioscience Odyssey Infrared Imaging System. Odyssey v3.0 software was used for quantification with linearity of measurement being confirmed using a standardisation bioassay with serial dilutions of sample inputs. Values of specific viral protein intensities were normalized against actin values. Primary antibodies included anti-ICP4 (Virusys, 1/1000); anti-ICP8 (1/2000); anti-VP5 (East Coast Bio, 1/3000), anti-HA (Invitrogen, 1/10,000), anti-pUL37 (a gift of P.Desai, 1/10,000), anti-pUL25 (a gift of V.Preston, 1/1000), LP1, anti-VP16 (1/4000, anti-VP1-2 (anti-NT1, 1/2000), anti-gB (1/10,000), anti-gD (a gift of G Cohen,1/10,000), anti-pUL6 (a gift from Arvind Patel, 1/1000) and monoclonal anti-actin (Sigma, 1/500).

RESULTS

Growth characteristics of K.VP1-2ΔNLS.

We previously identified a short, highly conserved basic motif in VP1-2, embedded within an otherwise poorly conserved region at the N-terminus of the protein (Figure 1a). We demonstrated that this motif could function as an efficient nuclear localisation signal (2). Further complementation assays with a mutant VP1-2 lacking the NLS indicated that it was important for virus growth. However definitive elucidation of its role requires the analysis of a virus lacking the motif. Therefore we constructed a mutant HSV KOS strain containing a short deletion of the 7 amino acids which provided the core NLS function (see materials and methods). Anticipating that this determinant would be important for virus growth we isolated and plaque purified the mutant virus on complementing cell lines (either HS30 or RSC-HAUL36) containing the wild-type (w/t) gene for VP1-2. The mutant replicated on the complementing cells, purified virus stocks were obtained and the deletion confirmed by sequencing across the UL36 gene. This virus designated K.VP1-2ΔNLS replicated only in complementing lines with plaque formation roughly comparable to the KOS w/t parental virus (Figure 1b,c). In striking contrast, in parallel assays in non-complementing Vero cells absolutely no plaque formation was observed and plaquing efficiency was decreased by at least 7 orders of magnitude compared to that on complementing cells (Figure 1b,c). Identical results were obtained when comparing plaque formation in complementing RSC-HAUL36 cells versus RSC cells (data not shown). Basically no plaques of any size were observed in Vero cells, RSC, Hep2 cells or any other cell type tested, though cpe was observed at high levels of virus inoculum. We next compared replication in multi-step growth curves in complementing versus non-complementing lines, assaying yield on complementing cells. Consistent with the lack of plaque formation, we observed a virtually complete absence of production of infectious virus (Figure 1d).

We also tested growth after high multiplicity infection in both Vero versus HS30 cells or RSC versus RSC-HAUL36 cells, with virus yields titred on the complementing cells. The results were similar in both situations and are shown in Figure 1e for Vero versus HS30. Growth of the KOS parental virus was approximately the same in both cell types. For K.VP1-2ΔNLS, while replication

kinetics and yields were similar to the parental virus in HS30 cells, yields in the non-complementing Vero cells were substantially delayed and reduced by an order of 3-4 logs (Figure 1e). Notwithstanding this reduction, it was clear that after the eclipse phase, infectious virus was produced from non-complementing cells after a high moi infection, that could infect and form plaques in complementing cells but not in non-complementing cells. Similar results were obtained in comparing RSC versus RSC-HAUL36 cells (data not shown).

To ensure that the profound phenotype of the mutant was due to the NLS deletion, we rescued K.VP1-2ΔNLS with w/t UL36, isolating the revertant termed K.VP1-2ΔNLS.R, and confirming restoration of the basic 7 amino acids by sequencing of purified viral DNA. The revertant could now propagate and plaque on any non-complementing cell type. A comparison of growth on non-complementing RSC cells demonstrating complete restoration of plaque formation is shown in (Figure S1a,b), with plaquing efficiencies now identical on non-complementing versus complementing cells. Plaque size for the revertant K.VP1-2ΔNLS.R was also comparable with that for the parental KOS w/t (Figure S1c). Protein expression, exemplified by ICP4 and ICP8 were restored in the revertant demonstrating progressive accumulation after low moi multi-step replication, unlike the virtual complete block for the mutant (Figure S1d). Taken together, the observation of complementation in cells containing UL36 and the reversion of phenotype by restoration of the basic motif, confirms that this 7 amino acid deletion of the NLS is the basis of the profound defect in replication and spread.

K.VP1-2ΔNLS, when amplified on complementing cells (which for ease of future reference we term K.VP1-2ΔNLS^{C}), clearly entered complementing cells and spread. We wished therefore to examine whether, although it could not form plaques at all, K.VP1-2ΔNLS^{C} could enter non-complementing cell types, with the defect in plaque formation being in some later aspect of propagation. To examine this we used serial dilutions in Vero cells similar to those in the plaque assays (Figure 1), but assaying by immunofluorescence to detect virus protein expression at the cell level. We observed that after 2-3 days when normal plaque formation for KOS w/t had spread and contained hundreds of infected cells, single antigen positive cells were observed for K.VP1-2ΔNLS^{C} (Figure 2a, arrows) but these cells showed no progression of infection to surrounding cells. Identical results showing bright antigen

positive single cells were obtained for a number of virus proteins, demonstrating firstly their expression and at the same time, lack of virus spread. Identical results, showing initial single infections and no spread, were obtained on a number of standard cell types including RPE, HFF and HaCaT (data not shown).

Considering the known recruitment of VP1-2 to virions, the reasonable interpretation of these results is that when K.VP1-2ΔNLS^{C} is propagated in complementing cells, the w/t VP1-2 from the cell line is recruited into virions which can then infect non-complementing cells, but in which further progression is profoundly blocked at one or more stages (see also below). To confirm the recruitment of w/t VP1-2, we analysed the expression of the w/t VP1-2 in the complementing cells, in this case in RSC-HAUL36 cells, during infection with K.VP1-2ΔNLS^{C}. This is made possible since the w/t VP1-2 in this line contains an HA-epitope tag enabling selective detection (52). The results show that while mock-infected RSC-HAUL36 cells expressed no detectable VP1-2.HA, infection with K.VP1-2ΔNLS^{C} induced the endogenous protein resulting in detectable levels from 12 h onwards (Figure 2b). We further analysed gradient purified extracellular virus particles of K.VP1-2ΔNLS^{C} (see below), demonstrating the presence of the HA-tagged w/t VP1-2 in the virions (Figure 2b, lane 10,11). These data confirm that, as expected, complementation is due to the incorporation of the w/t VP1-2 during propagation of K.VP1-2ΔNLS^{C}. It is possible that in complementing cells, the mutant VP1-2 is also recruited to virions in addition to the w/t protein but we cannot discriminate between the two proteins. The ΔNLS propagates in complementing cells while there is no spread at all in non-complementing cells. In the following series of experiments we addressed the key questions of whether, in non-complementing cells, particles were assembled and whether they contained the mutant VP1-2, (which in non-complementing cells could only be mutant VP1-2) and if these events occur, what was the nature of the profound block to virus spread.

Analysis of protein expression in K.VP1-2ΔNLS infected cells.

To that end we first examined various parameters of infection in non-complementing cells comparing K.VP1-2ΔNLS^{C} with the revertant K.VP1-2ΔNLS.R, during high moi infection (based upon titres obtained in complementing cells). First examining virus protein synthesis at 2-4 h intervals for 24 h, we observed virtually normal kinetics

and accumulation for representative immediate-early, early and late virus proteins, including in this latter class those proteins which have been shown to interact with VP1-2 (Figure 3a). No major differences were observed for a number of additional representative proteins including VP5, pUL37, pUL25 and the glycoprotein gD. For VP1-2 itself we noted a modest decrease in levels compared to infection with the revertant, though this would not be likely of itself to explain the profound phenotype in replication (see also below). We noted also in more refined analysis of the early part of infection, sampling every hour to 12 h, that there appeared to be a slight delay in accumulation of ICP4, though again this did not appear to have a significant effect on e.g., accumulation of ICP8 (Figure 3b) or other late proteins as indicated above.

Normal localisation of candidate virus proteins.

We also analysed localisation of candidate proteins after infection in non-complementing cells by immunofluorescence. Typical results obtained at 16 h post infection are shown in Figure 4. Generally expression and localisation of proteins including VP5, VP16, and pUL37 could not be differentiated between K.VP1-2ΔNLS^{C} and the revertant virus (Figure 4a). VP5 and VP16 were observed in nuclear patterns with accumulation in replication compartments with additional cytoplasmic VP16, as previously reported. pUL37 was also observed in a cytoplasmic pattern that could not be differentiated between mutant and revertant. For VP1-2 itself, we have previously reported on localisation in infected Vero cells showing that although the protein contains an NLS, the majority was found in the cytoplasm, though with a discernible minor population in the nucleus (2). Interestingly in this current work in RSC cells, we found little evidence for a population of nuclear VP1-2, detecting mainly a cytoplasmic pattern, frequently in a perinuclear or aggregated pattern, though the comparatively rapid rounding up of infected RSC cells made localisation studies more difficult (Figure 4b). Nevertheless we found little difference in localisation of VP1-2 comparing infection with the mutant and revertant viruses. To further examine whether we could detect any difference in VP1-2 we also examined localisation in infected Vero cells (Figure 4b). In this case, again while the majority of the protein was in the cytoplasm frequently in large perinuclear punctae, we could now detect a population of nuclear VP1-2 as previously reported. Indeed a

discernible difference was now observed, with K.VP1-2ΔNLS exhibiting little detectable nuclear VP1-2. This result serves to illustrate a potential phenotype of the NLS deletion on de novo synthesised VP1-2, at least where nuclear VP1-2 can be detected. However such a difference was not readily discernible in RSC cells neither in other cell types analysed such as HaCaT (data not shown), where clearly the w/t virus could replicate normally but without significant levels of nuclear VP1-2. We do not know the reason for the cell type difference in VP1-2 location but possible explanations include differences in VP1-2 cleavage or non-specific breakdown in different cells. A comprehensive analysis of the localisation of all virus encoded proteins, ultimately aimed at addressing virion formation in K.VP1-2ΔNLS is beyond the scope of this work and tractability. However within the limits for these types of analyses, the results indicate normal expression levels and localisation for a series of representative proteins. Moreover such a comprehensive analysis is rendered unnecessary in the light of additional results below.

Virion assembly during infection by K.VP1-2ΔNLS.

Based on the results above, the profound defect in K.VP1-2ΔNLS^{C} when infecting non-complementing cells is clearly at a stage after initial infection. Considering the observations of normal protein synthesis, at least of all candidates examined including late proteins, the next key question was whether capsids and virions would be assembled at all during infection with the mutant, with the defect being at some stage downstream of this, or whether the deletion of the motif in VP1-2 prevented some late stage of assembly itself. To address this, we first performed electron microscopy (EM) analyses of non-complementing cells infected by the mutant in comparison to the w/t virus. The results (Figure 5) generally indicated little discernible difference between the mutant and w/t virus. Importantly formation of full capsids was observed in the nucleus of cells infected with K.VP1-2ΔNLS (Figure 5a, arrows) and the w/t virus (Figure 5d, arrows). Cytosolic capsids were also observed either as free capsids but also in membrane wrapping intermediates, examples of which are shown (Figure 5b,e, arrows). Finally, enveloped particles were also observed at the cell surface for both K.VP1-2ΔNLS and the w/t virus (Figure 5c,f). Additional examples showing readily detectable cell surface or extracellular enveloped virions for the K.VP1-2ΔNLS mutant are show in panels g,h. Over the

course of this work, we could detect no significant difference in capsid or enveloped particle formation in the nucleus and cytoplasm between the mutant and w/t virus (see additional data below). Clearly these data indicate that the profound defect in ΔNLS propagation is not due to a defect in the known requirement for VP1-2 for virion assembly per se. They also demonstrate that the deletion did not affect the global folding and functioning of the protein, since VP1-2 is known to be essential for assembly and for multiple interactions necessary for this complex activity. Given that we could now observe virion formation and extracellular virus after infection by K.VP1-2ΔNLS^{C} in non-complementing (i.e., UL36 –ve) cells, we termed such virions K.VP1-2ΔNLS^{NC}.

Extracellular virion formation by K.VP1-2ΔNLS.

From the observations of on the one hand, the profound defect in spread seen after low multiplicity infection, while on the other hand the very similar levels of protein expression and the formation of enveloped virions, the implication of our studies was that K.VP1-2ΔNLS^{NC} extracellular virions were formed but would be blocked at some stage of subsequent infection in secondary cells. We next performed a more quantitative analysis of virion production and infectivity. Since multi-round virion production was impossible, we performed high moi infections in non-complementing cells (in this case HaCaT human keratinocytes, which from comparative analysis generally produced increased yields of all HSV-1 strains). Cells were infected with the mutant or revertant virus at a moi of 1 (based in titres in complementing cells) and the media harvested at 16 h post infection. The media was clarified and extracellular virus then pelleted and analysed firstly by SDS gel electrophoresis and total protein staining. The results showed similar levels of extracellular virion production. When normalised for levels of major capsid protein by minor adjustment little significant difference in qualitative or quantitative terms could be observed between the virion protein profiles (Figure 6a). In particular there was no difference in the relative abundance of VP1-2 itself, e.g., compared to major capsid protein VP5. Further analysis by western blotting of a number of structural proteins including VP5, VP1-2, pUL37, VP16, pUL25, gB and pUL6 also showed little difference between the mutant and revertant particles (Figure 6b). Without a complete comprehensive analysis of all virus (and host) proteins, and their potential

modifications, it is formally impossible to state that there were no qualitative differences in the protein profiles of the mutant and revertant particles (with the implication that the deletion of NLS of VP1-2 was responsible for any proposed differences). However within the limitations of SDS-PAGE and Western blot analysis of extracellular particles, we could not detect significant differences between the mutant and revertant protein profiles of extracellular virions. We further analysed these extracellular particles by negative staining observing at least as many particles from the K.VP1-2ΔNLS infected medium. While inherent in such analysis, stain penetration is not homogeneous and a range of particles are observed, no significant differences were detected between the mutant and revertant. Sample images showing stained particles for the mutant and revertant samples are shown in Figure 6c. Taking altogether with the thin section EM analysis and expression data, these data demonstrate little defect in virion assembly and release of K.VP1-2ΔNLS.

In contrast, there was a very considerable difference in infectivity. Normalising for major capsid protein in the extracellular virus preparations, infectious titres of the mutant virus, (analysed by titration in complementing HS30 cells), was of the order of 1000-fold lower than the revertant (Figure 6d). This result is consistent with the initial analytical scale analysis (Figure 1), where despite a complete block in spread after single cell infection, some infectious virus was produced after high moi infection but at approximately 1000-fold lower efficiency. The implications of the current EM and extracellular virus analyses, are that this decrease is not due to a defect in the production of virus particles, but rather that such particles are produced and are profoundly reduced in their ability to initiate infection in a new cell.

Block to infection in K.VP1-2ΔNLS^{NC}.

To characterise the block to infection further we next examined the mutant virus now made in non-complementing cells, i.e., K.VP1-2ΔNLS^{NC}, in low multiplicity infections in non-complementing cells, identifying successfully infected cells by immunofluorescence similar to that shown in Figure 2. The implication of our results in the previous section would be that with standardised amounts of infecting particles, the numbers of cells initiating infection would be considerably reduced in the mutant compared to the w/t virus. We infected Vero or HS30 cells with a series of dilutions of the extracellular virus preparations, standardised on major capsid protein

(which we generally found more consistent than particle counts) and designed to give 1/1000, 1/100 to 1/3 cells infected (based on titres of the revertant virus) and enumerated antigen positive cells in multiple fields for the revertant and NLS mutant. Typical fields shown are Vero cells with the highest amount of input virus which emphasises the difference in infectivity between the revertant and mutant (Figure 6e). At this input, evaluating 1392 cells in several fields, 398 were positive for ICP4 protein synthesis for the revertant virus. An approximately 2-fold higher rate of infection was observed in HS30 cells (Figure 6f). In striking contrast for the mutant evaluating 1685 cells no positive cells were detected in Vero cells and of 1442 HS30 cells, 8 were positive for ICP4 (Figure 6f).

We also examined infection at nominally higher multiplicities and examined protein synthesis by Western blotting (Figure 6g). We infected cells with virus purified from extracellular medium, at an input of 5 pfu/cell (based on titres of the revertant) or equal input inoculum for the mutant again standardised on VP5 capsid protein levels. The results demonstrated that while we could readily detect e.g. ICP8 or VP5 protein synthesis for the revertant, we detected little protein synthesis for the VP1-2.ΔNLS mutant, with only minor amounts of these proteins observed very late after infection (Figure 6g). Altogether these data demonstrate a profound block to infection by K.VP1-2ΔNLS^{NC} particles.

There could be several explanations for the block in K.VP1-2ΔNLS^{NC} infection including virus entry to the cells or some block in virus gene expression per se. Such explanations would invoke a critical role of the NLS of VP1-2 in assembly of a particle that would fuse normally (which while formally possible seemed less likely to us) or a role of the NLS in immediate early expression per se, which also seemed less likely. Given the strong evidence from previous analysis for a role of VP1-2 in transport to and docking with the nuclear pore (1, 4, 31, 52), it seemed reasonable to propose that disruption in some aspect of the early intracellular pathway may underpin the defect in K.VP1-2ΔNLS^{NC}.

To that end we next examined localisation of infecting capsids in cells infected with K.VP1-2ΔNLS^{NC} or the revertant by immunofluorescence (Figure 7) and by electron microscopy (Figure 8,9). We wished to address the questions of whether K.VP1-2ΔNLS^{NC} particles entered cells, and if so where the apparent block to infection may be. For these localisation studies, multiple images were collected in

the Z-dimension and images compiled to give an accurate representation throughout the cell. Cells were infected as before with extracellular virus, in this case at a moi of 100 for the revertant or with a standardised input of K.VP1-2ΔNLS^{NC}. After infection at +4^{0}C the cells were washed, warmed to 37^{0}C and incubated for 2 or 4 h. At these times the cultures were fixed, permeabilised and stained with anti-VP5 antibody. In parallel control infections, cells were maintained at +4^{0}C to prevent virus entry. This analysis showed a distinct difference in the behaviour of the mutant and revertant particles.

For the revertant virus, after shifting to 37^{0}C particle staining at 2 h was distinct from that seen at +4^{0}C, with numerous cytoplasmic particles reflecting particle internalisation (Figure 7a, panels I,II). By 4h virtually all the cells also now exhibited homogeneous nuclear staining reflecting successful infection, gene expression and de novo synthesis of VP5 (Figure 7a, panel III,IV), the latter being absent when analysis was performed in the presence of cycloheximide (data not shown). Considering that virtually all the cells were successfully infected by the revertant and synthesising VP5 (Figure 7a, panel IV), it was surprising that we could not see abundant nucleocapsid aggregation around the nuclear rim, though individual particle association could be observed. Nevertheless a clear difference was observed with the ΔNLS mutant, though not what we had originally anticipated. For the mutant virus, the pattern was clearly different at 37^{0}C compared to +4^{0}C, reflecting capsid internalisation (Figure 7a, panels V,VI). However by 2 h the pattern for the mutant could now be distinguished from the revertant and this became even more pronounced at 4 h. Thus the ΔNLS mutant was seen congregating in distinct accumulations in a single perinuclear region, and though capsids were clearly internalised (see also EM analysis below), none of the cells exhibited the diffuse nuclear VP5 indicative of de novo synthesis. This pronounced difference in behaviour between the revertant and mutant virus is clear in panels IV versus VIII which omits the nuclear counterstain. The perinuclear accumulation of the mutant was observed in many cells (Figure 7, panel VIII, indicated by arrows) and was reminiscent of congregation around the microtubule organising centre (MTOC). That the distinct localisation of the ΔNLS capsids represented congregation around the MTOC is confirmed in Figure 7b (panel I, see also Figure S2) showing a confocal section, this time co-stained with anti-PCM1, one of a class of centriolar specific

proteins which associates with cytoplasmic granules and concentrates around the MTOC and centriolar matrix (12). The extent of congregation was quantified for revertant and mutant capsids. Defined and unbiased areas of interest (2 μm diameter circles) were applied around PCM1 foci, and the accumulated density of pixels in the green VP5 channel in the same areas then calculated. We evaluated multiple fields and approximately 130 cells for each virus (Figure 7c, each vertical bar represents a cell). While a congregation pattern could be observed in some cells for the revertant virus, the distinction in behaviour in MTOC association between the two viruses was very clear. We found that a pixel density of approximately 2000 by quantitative analysis corresponded to the classification as a cluster by visual inspection. Using this value as a threshold to aid comparison, approximately 10% of the cells showed MTOC clustering for the revertant as compared to 75% for the mutant, though this represents a conservative estimate of the difference in behaviour which was highly significant ($p<0.0001$).

The simplest explanation for our results is that the block in VP1-2ΔNLS capsid transport to the nucleus could be due to a requirement for the VP1-2 NLS for capsid interactions with cellular machinery. However, formally it could be that the requirement for the NLS reflected its involvement in retaining VP1-2 on the capsid during entry, in order for it to carry out some other function. Considering that the NLS was not required for VP1-2 recruitment and virus assembly this seems less likely in our view. However such a scenario has been proposed for a C-terminal determinant of VP1-2 (53). We therefore examined VP1-2 presence during infection by K.VP1-2ΔNLS in confocal z sections stained with combinations of antibodies. Since our anti-VP5 and anti-VP1-2 combination was not suitable we stained with either anti-VP5 and pUL37 or anti-VP1-2 and pUL37 combinations. The results showed the almost quantitative association of pUL37 with VP5+ve capsids and the same association for VP1-2 with pUL37+ve capsids (Figure 7b, panels II and III). These data indicate that VP1-2 remains on incoming capsids during infection with K.VP1-2ΔNLS and that the requirement for the NLS more likely reflects a direct involvement in capsid targeting.

To pursue the defect in K.VP1-2ΔNLS capsid entry, we performed a similar analysis using electron microscopy of thin sections (70 nm) after high moi infection of the mutant and revertant. For both the revertant and mutant, we readily observed internalised capsids, free of membranes in the cytosol of infected cells (Figure 8, 9).

However, consistent with the immunofluorescence analysis, a key qualitative difference was observed between the two, quantified in Figure 9c. The perimeter of nuclear envelope (NE) of 100 cells was scanned and scored for capsids in close proximity to the NE (within approximately 100 nm) and also classed as empty or DNA-containing capsids. For the revertant virus we could detect such capsids, typical examples of which are shown in Figure 8 with approximately 85% of these being empty and the majority adjacent to pore structures (Figure 9c). In contrast, for K.VP1-2 ΔNLS, capsids in close proximity to the NE were rare and what few were observed retained DNA and were not associated with pores (Figure 9c). Instead we observed capsids, frequently in close proximity to the centrioles within the microtubule organising centre, not wrapped in membranes and all containing DNA. Figure 9 a,b shows an example field with multiple full capsids (small arrowheads) in close proximity to the centriole (large single arrowhead). Taken together these data answer several questions. Firstly they show that ΔNLS virions, which exhibit a profound block in infection, were able to enter cells. Moreover, although at the EM level it is difficult to be categorical, nevertheless we could not identify ΔNLS empty capsids in proximity to the nuclear pore. Altogether, with the distinct phenotype and more quantitative analysis of capsid localisation by immunofluorescence and the clear failure to initiate gene expression, the most reasonable explanation for our data is that the ΔNLS mutant exhibits a major block in forward routing from the MTOC and/or docking with the nuclear pore, resulting in a profound block to the normal progression of infection. These data provide evidence that the short NLS at position 475 in VP1-2, which exhibits strong positional and sequence conservation in the homologues in all herpesviruses (2), is critical for virus spread and further that while dispensable for virion assembly per se, is key to normal entry early in infection via routing to the nuclear pore.

DISCUSSION

Herpesvirus capsids must navigate the cytosolic environment of the cells which they infect, dock and engage with nuclear pores, and deposit their genomes across the pore for subsequent gene expression. Any mechanistic understanding of these early pathways requires the identification and dissection of the virus and host proteins involved. However most of the potential virus candidates for an important

role in early entry are essential proteins required for virus assembly. Thus their complete deletion results in failure to assemble a particle and prevents any further detailed analysis of a specific role in entry and the mechanism involved. VP1-2 is conserved in all herpesviruses and is absolutely essential for virus assembly (13, 15, 34, 52). However strong evidence for an additional role of VP1-2 in entry was provided from previous data on the retention of a subset of tegument proteins including VP1-2 on infecting capsids (19, 23, 30, 37, 39, 40, 45, 51, 56, 61), on the failure of VP1-2-ve capsids to infect nuclei in polykaryocytes (52), and on a ts defect in entry mapping to VP1-2 (1, 5, 31). Nevertheless any mechanistic understanding of the relevant pathways and the role of VP1-2 requires identification of variants wherein virion assembly and secondary infection still occur, yet virus propagation is defective. Here we construct and characterise a variant in which infection and virus assembly proceeds but virus propagation and cell to cell spread is profoundly blocked. A summary of the features of this virus mutant is illustrated schematically in Figure 10. Taken together our data provide strong support for the proposal that the basic motif of VP1-2 functions as an NLS to promote successful transport to and/or interaction with nuclear pore complexes and that this is a critical requirement for successful infection.

There could be several not mutually exclusive explanations to account for our observations since distinct events in transport, docking or subsequent to nuclear pore engagement can all be involved in early nuclear entry (60). While VP1-2 has been shown to be required for intracellular microtubule-mediated capsid transport (38, 55, 61), our results indicate that a defect in the initial interaction and transport of the VP1-2ΔNLS mutant capsid, at least from the periphery of the cell, would not be the most likely explanation for the block in infection. Although defects in early transport mechanisms, e.g., in peripheral interactions or in the kinetic efficiency of transport to the interior of the cell, are less likely explanations and not supported by current data, they will be addressed formally in future work when a fluorescent derivative of the VP1-2ΔNLS mutant can be constructed.

It could have been that capsids were transported to the pore without a requirement for the VP1-2 NLS (but with a requirement for other specific capsid/tegument determinants), with the NLS being involved in promoting tight engagement with the pore or a key event subsequent to pore interaction per se. For

example, in adenovirus, capsid binding to nuclear pores has been reported to be independent of importin and presumably of any NLS motifs in capsid proteins, and mediated instead by direct capsid binding to pore components including Nup214 (58). However our data support a role for VP1-2 NLS interactions specifically in routing to the pore, though there could be several not mutually exclusive explanations regarding the detailed processes involved. For example while not required for peripheral transport, it could be that the NLS is required for promoting subsequent transport of capsids directly, i.e. with the NLS determinant directly interacting with the cytoskeleton associated transport machinery, or indirectly by binding some type of NLS receptor, e.g., an importin and by virtue of this interaction, promoting transport to the pore. It could also be that the NLS is involved in capsid detachment from microtubules after retrograde transport and indeed it is possible that these events are coupled (see below).

It has previously been reported that HSV virions stripped of their envelope by detergent extraction, could bind to nuclear pores in vitro (46). Such in vitro binding could be inhibited to some degree either by a general broad antibody to multiple nucleoporins or by antibody to importin β and importin β was reported to be sufficient to promote capsid binding to isolated nuclei (46). No specific virus receptors were identified for such binding, but mild trypsin treatment of the capsids, removing several tegument proteins including VP13/14, VP22, VP16, and VP1-2 was reported to inhibit capsid-nuclear interaction. Also antibody to VP1-2 itself, when scrape loaded into cells resulted in a reduction in capsid accumulation at the nuclear pore (11). It is tempting to speculate that the pronounced requirement for the NLS of VP1-2 we now demonstrate could reflect an involvement of importin β. However it was also reported that importin α, which directly interacts with NLS motifs (17, 18) did not support capsid binding, and that an NLS-peptide conjugate could not compete for capsid-pore docking. This would imply that the VP1-2 NLS did not bind importin α but rather had specificity for importin β. Moreover, antibody to nucleoporins (46) also inhibited capsid binding in vitro and siRNA knockdown of nucleoporins reduced capsid accumulation at the nucleus in vivo (11). These effects though modest indicate that other interactions may be involved in capsid-pore interactions (see below).

The distinct congregation of the ΔNLS mutant capsids around the MTOC and our failure to detect any empty capsids around the pore indicate that the NLS somehow promotes the forward routing of capsids from the MTOC and/or the detachment from the MTOC or surrounding region. The most straightforward explanation is that, without any necessary spatial restriction, the VP1-2NLS interacts with a cellular component as it undergoes retrograde transport to the interior of the cell retaining the component on the virus capsid. Some downstream event, possibly but not necessarily involving the NLS, then promotes release or alteration of the capsid and transport towards the pore dependent upon VP1-2 and its NLS associated component(s). This explanation would not rule out additional downstream roles for the NLS once docked at the pore. The congregation of the ΔNLS mutant around the MTOC would then be a result of the inefficient directed transport towards the pore and/or an actual retention of the ΔNLS capsids within and around the MTOC region.

It is also possible that the NLS functions or interacts with its potential receptor in a spatially restricted way once at the MTOC, a region known to have particular structure and a matrix like organisation (12, 26, 33). One explanation for this could a regulated conformational exposure such as is thought to occur on the capsid of hepatitis B virus (HBV). HBV capsids (from bacterially expressed core protein), bind nuclear pores at least in permeabilized cells dependent upon phosphorylation at residues adjacent to an NLS motif. It is proposed that phosphorylation exposes the NLS for importin binding and pore docking (27). It could be that the disposition or activity of the VP1-2 NLS is regulated, either to promote exposure and function in entry, or to mask or inhibit its activity later after de novo synthesis and incorporation into newly assembled capsids during exit. An example of an event which might promote function or presentation of the NLS would be in proteolytic cleavage of VP1-2 which one report has indicated may be relevant at some stage of early infection (25).

Furthermore it is intriguing that in certain circumstances e.g., for intra-axonal transport, certain importin species have been shown to be complexed with the retrograde motor dynein. Signalling pathways induce the rapid translation of spatially restricted importin β mRNA into protein that is distant from the cell body and then complexes with importin α and dynein to enable nuclear translocation of cargo (22,

48). By this manner it is possible that an NLS acts as a determinant both for microtubule-associated transport, and nuclear pore interaction. While such a mechanism is possible, it is more plausible for the neurotropic herpesviruses. Other mechanisms not requiring spatially restricted NLS interactions are more likely to explain the requirement for the VP1-2 NLS in core replication pathways in culture. Thus the NLS motif could be engaged at any of a number of points, but be critically important in forward transport from the MTOC area.

Clearly other determinants in VP1-2 are also critical for virus replication. Insertional and deletion mutations in several regions abrogate VP1-2 function. Little is known about the basis of the VP1-2 disruption, though it is likely that such mutants will affect the known essential roles of VP1-2 in recruiting additional tegument proteins in the assembly pathway. Indeed certain mutants have been shown to specifically disrupt VP1-2 interactions with other tegument proteins required for assembly (7, 15, 29, 32, 34, 41, 42). One specific VP1-2 determinant, the extreme carboxy terminal region, promotes with the essential capsid protein pUL25 (8, 34). In pseudorabies virus, deletion of the extreme C-terminal 23 residues abrogates virus replication (34, 42), an effect which has been attributed to disruption of VP1-2 recruitment to capsid possibly by direct interaction with pUL25 (10, 47). Since pUL25 itself has also been implicated in early events during the initiation of infection (47, 49) clearly such additional VP1-2 determinants could play a role in entry events. Indeed it has previously been shown that pUL25 when expressed individually could bind nucleoporins, and thus it has been proposed that it could act on capsids as an interface with the nuclear pore (47). If this were the case, from our results it would be insufficient to promote nuclear pore engagement in the absence of the VP1-2 NLS. Nevertheless it remains possible that VP1-2 plays a role in promoting pUL25 function after docking. It could for example be that downstream of NLS-promoted routing to the pore, the NLS itself or additional determinants in VP1-2 and/or pUL25 engage with specific pore components such as Nup214 or Nup358. However the role of C-terminus of VP1-2 may be more complicated than first anticipated since recent results indicate that the C-terminal is not required for VP1-2 function in virion assembly, but rather is specifically required to retain the protein on capsids as it infects secondary cells (53). This apparently indicates that VP1-2 remains bound to newly formed capsids and promotes virion assembly without requiring the C-terminal pUL25–interacting region, but detaches from capsids after they infect cells if this C-

terminal region is not present. This determinant appears to act in a distinct fashion from the NLS identified here.

In conclusion our results advance understanding of the role of VP1-2 specifically in entry pathways of HSV. The characterisation of the phenotype and the nature of block to entry uncouple critical determinants in VP1-2 for early intracellular routing pathways. These results provide a framework for future detailed analysis of the host cell factors involved, since these can be linked to a physiologically relevant and critical determinant whose alteration has a profound phenotype. Furthermore, considering the conserved and essential nature of VP1-2 and presence of the basic NLS-like motif in a similar position in all homologues (2), we believe that this motif may play a similar critical role in other herpesvirus species. Finally, in principle targeting the function of the NLS could provide a useful therapeutic avenue and the debilitated virus itself could prove useful in other settings such as gene therapy where entry is required but second round spread not desirable, or in vaccine applications.

Acknowledgements

We thank Fraser Rixon and Valerie Preston for antibodies and cells, Prashant Desai for the complementing cell line HS30. We thank Tomi Kuyoro for help with virus titrations. We are grateful to David Leib for provision of the KOS bacmid, and to Nick Osterrieder and Greg Smith for Bacmid reagents. We thank Martin Spitaller for assistance with confocal microscopy. C.M.C. was supported by a University Research Fellowship from the Royal Society. FA was in receipt of a fellowship from the Spanish Ministerio de Educacion y Ciencia. This work was funded by Marie Cure Cancer Care.

REFERENCES

1. **Abaitua, F., T. Daikoku, C. M. Crump, M. Bolstad, and P. O'Hare.** 2011. A single mutation responsible for temperature sensitive entry and assembly defects in the VP1-2 protein of HSV. Journal of virology **85:**2024-2036.
2. **Abaitua, F., and P. O'Hare.** 2008. Identification of a highly conserved, functional nuclear localization signal within the N-terminal region of herpes simplex virus type 1 VP1-2 tegument protein. J. Virol. **82:**5234-5244.
3. **Abaitua, F., R. N. Souto, H. Browne, T. Daikoku, and P. O'Hare.** 2009. Characterization of the herpes simplex virus (HSV)-1 tegument protein VP1-2

during infection with the HSV temperature-sensitive mutant tsB7. J. Gen. Virol. **90:**2353-2363.

4. **Batterson, W., D. Furlong, and B. Roizman.** 1983. Molecular genetics of herpes simplex virus. VIII. further characterization of a temperature-sensitive mutant defective in release of viral DNA and in other stages of the viral reproductive cycle. J. Virol. **45:**397-407.
5. **Batterson, W., and B. Roizman.** 1983. Characterization of the herpes simplex virion-associated factor responsible for the induction of alpha genes. J. Virol. **46:**371-377.
6. **Bolstad, M., F. Abaitua, C. M. Crump, and P. O'Hare.** 2011. Autocatalytic activity of the Ubiquitin Specific Protease domain of HSV-1 VP1-2. Journal of virology **85:**8738-8751.
7. **Bottcher, S., H. Granzow, C. Maresch, B. Mohl, B. G. Klupp, and T. C. Mettenleiter.** 2007. Identification of functional domains within the essential large tegument protein pUL36 of pseudorabies virus. J. Virol. **81:**13403-13411.
8. **Bottcher, S., B. G. Klupp, H. Granzow, W. Fuchs, K. Michael, and T. C. Mettenleiter.** 2006. Identification of a 709-amino-acid internal nonessential region within the essential conserved tegument protein (p)UL36 of pseudorabies virus. Journal of virology **80:**9910-9915.
9. **Cohen, S., S. Au, and N. Pante.** 2011. How viruses access the nucleus. Biochimica et biophysica acta **1813:**1634-1645.
10. **Coller, K. E., J. I. Lee, A. Ueda, and G. A. Smith.** 2007. The capsid and tegument of the alpha herpesviruses are linked by an interaction between the UL25 and VP1-2 proteins. J.Virol. **81:**11790-11797.
11. **Copeland, A. M., W. W. Newcomb, and J. C. Brown.** 2009. Herpes simplex virus replication: roles of viral proteins and nucleoporins in capsid-nucleus attachment. Journal of virology **83:**1660-1668.
12. **Dammerman, A., and A. Merdes.** 2002. Assembly of centrosomal proteins and microtubule organization depends on PCM-1. J. Cell Biol. **159:**255-266.
13. **Desai, P. J.** 2000. A null mutation in the UL36 gene of herpes simplex virus type 1 results in accumulation of unenveloped DNA-filled capsids in the cytoplasm of infected cells. J. Virol. **74:**11608-116018.
14. **Flint, S. J., L. W. Enquist, R. M. Krug, V. R. Racaniello, and A. M. Skalka.** 2009. Principles of Virology. ASM Press, Washington DC.
15. **Fuchs, W., B. G. Klupp, H. Granzow, and T. C. Mettenleiter.** 2004. Essential function of the pseudorabies virus UL36 gene product is independent of its interaction with the UL37 protein. J. Virol. **78:**11879-11889.
16. **Gierasch, W. W., D. L. Zimmerman, S. L. Ward, T. K. VanHeyningen, J. D. Romine, and D. A. Leib.** 2006. Construction and characterisation of bacterial artifical chromosomes containing HSV-1 strains 17 and KOS. J. Virol. Methods **135:**197-206.
17. **Goldfarb, D. S., A. H. Corbett, D. A. Mason, M. T. Harreman, and S. A. Adam.** 2004. Importin alpha: a multipurpose nuclear-transport receptor. Trends in cell biology **14:**505-514.
18. **Gorlich, D., and U. Kutay.** 1999. Transport between the cell nucleus and the cytoplasm. Annual review of cell and developmental biology **15:**607-660.
19. **Granzow, H., B. G. Klupp, and T. C. Mettenleiter.** 2005. Entry of pseudorabies virus: an immunogold-labeling study. J. Virol. **79:**3200-3205.

20. **Greber, U. F., and A. Fassati.** 2003. Nuclear import of viral DNA genomes. Traffic **4:**136-143.
21. **Greber, U. F., and M. Fornerod.** 2005. Nuclear import in viral infections. Current topics in microbiology and immunology **285:**109-138.
22. **Hanz, S., E. Perlson, D. Willis, J. Q. Zheng, R. Massarwa, J. J. Huerta, M. Koltzenburg, M. Kohler, J. van-Minnen, J. L. Twiss, and M. Fainzilber.** 2003. Axoplasmic importins enable retrograde injury signaling in lesioned nerve. Neuron **40:**1095-1104.
23. **Heine, J. W., R. W. Honess, E. Cassai, and B. Roizman.** 1974. Proteins specified by herpes simplex virus XII. The virion polypeptides of Type 1 strains. J. Virol. **14:**640-651.
24. **Jarosinski, K., L. Kattenhorn, B. Kaufer, H. Ploegh, and N. Osterrieder.** 2007. A herpesvirus ubiquitin-specific protease is critical for efficient T cell lymphoma formation. Proc. Natl. Acad. Sci. USA **104:**20025-20030.
25. **Jovasevic, V., L. Liang, and B. Roizman.** 2008. Proteolytic cleavage of VP1-2 is required for release of herpes simplex virus 1 DNA into the nucleus. J. Virol. **82:**3311-3319.
26. **Kalt, A., and M. Schliwa.** 1993. Molecular components of the centrosome. Trends in cell biology **3:**118-128.
27. **Kann, M., B. Sodeik, A. Vlachou, W. H. Gerlich, and A. Helenius.** 1999. Phosphorylation-dependent binding of hepatitis B virus core particles to the nuclear pore complex. The Journal of cell biology **145:**45-55.
28. **Kattenhorn, L. M., G. A. Korbel, B. M. Kessler, E. Spooner, and H. L. Ploegh.** 2005. A deubiquitinating enzyme encoded by HSV-1 belongs to a family of cysteine proteases that is conserved across the family Herpesviridae. Mol. Cell. **19:**547-557.
29. **Kelly, B. J., E. Diefenbach, C. Fraefel, and R. J. Diefenbach.** 2012. Identification of host cell proteins which interact with herpes simplex virus type 1 tegument protein pUL37. Biochemical and biophysical research communications **417:**961-965.
30. **Klupp, B. G., W. Fuchs, H. Granzow, R. Nixdorf, and T. C. Mettenleiter.** 2002. Pseudorabies virus UL36 tegument protein physically interacts with the UL37 protein. Journal of virology **76:**3065-3071.
31. **Knipe, D. M., W. Batterson, C. Nosal, B. Roizman, and A. Buchan.** 1981. Molecular genetics of herpes simplex virus. VI. Characterization of a temperature-sensitive mutant defective in the expression of all early viral gene products. J. Virol. **38:**539-547.
32. **Ko, D. H., A. L. Cunningham, and R. J. Diefenbach.** 2011. The major determinant for addition of tegument protein pUL48 (VP16) to capsids in herpes simplex virus type 1 is the presence of the major tegument protein pUL36 (VP1/2). Journal of virology **84:**1397-1405.
33. **Kollman, J. M., A. Merdes, L. Mourey, and D. A. Agard.** 2011. Microtubule nucleation by gamma-tubulin complexes. Nature reviews. Molecular cell biology **12:**709-721.
34. **Lee, J. I., G. W. Luxton, and G. A. Smith.** 2006. Identification of an essential domain in the herpesvirus VP1/2 tegument protein: the carboxy terminus directs incorporation into capsid assemblons. J. Virol. **80:**12086-12094.

35. **Lee, J. I., P. J. Sollars, S. B. Baver, G. E. Pickard, M. Leelawong, and G. A. Smith.** 2009. A Herpesvirus Encoded Deubiquitinase Is a Novel Neuroinvasive Determinant. PLoS pathogens **5:**e1000387.
36. **Levin, A., A. Loyter, and M. Bukrinsky.** 2011. Strategies to inhibit viral protein nuclear import: HIV-1 as a target. Biochimica et biophysica acta **1813:**1646-1653.
37. **Luxton, G. W., S. Haverlock, K. E. Coller, S. E. Antinone, A. Pincetic, and G. A. Smith.** 2005. Targeting of herpesvirus capsid transport in axons is coupled to association with specific sets of tegument proteins. Proceedings of the National Academy of Sciences of the United States of America **102:**5832-5837.
38. **Luxton, G. W., J. I. Lee, S. Haverlock-Moyns, J. M. Schober, and G. A. Smith.** 2006. The pseudorabies virus VP1/2 tegument protein is required for intracellular capsid transport. J. Virol. **80:**201-209.
39. **Mettenleiter, T.** 2002. Herpesvirus asembly and egress. J.Virol. **76:**1537-1547.
40. **Michael, K., B. G. Klupp, T. C. Mettenleiter, and A. Karger.** 2006. Composition of pseudorabies virus particles lacking tegument protein US3, UL47, or UL49 or envelope glycoprotein E. Journal of virology **80:**1332-1339.
41. **Mijatov, B., A. L. Cunningham, and R. J. Diefenbach.** 2007. Residues F593 and E596 of HSV-1 tegument protein pUL36 (VP1/2) mediate binding of tegument protein pUL37. Virology **368:**26-31.
42. **Mohl, B. S., S. Bottcher, H. Granzow, W. Fuchs, B. G. Klupp, and T. C. Mettenleiter.** 2010. Random transposon-mediated mutagenesis of the essential large tegument protein pUL36 of pseudorabies virus. J. Virol. **84:**8153-8162.
43. **Mohl, B. S., S. Bottcher, H. Granzow, J. Kuhn, B. G. Klupp, and T. C. Mettenleiter.** 2009. Intracellular localization of the pseudorabies virus large tegument protein pUL36. Journal of virology **83:**9641-9651.
44. **Monette, A., N. Pante, and A. J. Mouland.** 2011. HIV-1 remodels the nuclear pore complex. The Journal of cell biology **193:**619-631.
45. **Newcomb, W. W., and J. C. Brown.** 2010. Structure and Capsid Association of the Herpesvirus Large Tegument Protein UL36. J.Virol. **doi:10.1128**.
46. **Ojala, P. M., B. Sodeik, M. W. Ebersold, U. Kutay, and A. Helenius.** 2000. Herpes simplex virus type 1 entry into host cells: reconstitution of capsid binding and uncoating at the nuclear pore complex in vitro. Molecular and cellular biology **20:**4922-4931.
47. **Pasdeloup, D., D. Blondel, A. L. Isidro, and F. J. Rixon.** 2009. Herpesvirus capsid association with the nuclear pore complex and viral DNA release involve the nucleoporin CAN/Nup214 and the capsid protein pUL25. Journal of virology **83:**6610-6623.
48. **Perry, R. B., and M. Fainzilber.** 2009. Nuclear transport factors in neuronal function. Seminars in cell & developmental biology **20:**600-606.
49. **Preston, V. G., J. Murray, C. M. Preston, I. M. McDougall, and N. D. Stow.** 2008. The UL25 gene product of herpes simplex virus type 1 is involved in uncoating of the viral genome. Journal of virology **82:**6654-6666.
50. **Rabe, B., M. Delaleau, A. Bischof, M. Foss, I. Sominskaya, P. Pumpens, C. Cazenave, M. Castroviejo, and M. Kann.** 2009. Nuclear entry of hepatitis

B virus capsids involves disintegration to protein dimers followed by nuclear reassociation to capsids. PLoS pathogens **5:**e1000563.

51. **Radtke, K., D. Kieneke, A. Wolfstein, K. Michael, W. Steffen, T. Scholz, A. Karger, and B. Sodeik.** 2010. Plus- and minus-end directed microtubule motors bind simultaneously to herpes simplex virus capsids using different inner tegument structures. PLoS pathogens **6:**e1000991.
52. **Roberts, A. P., F. Abaitua, P. O'Hare, D. McNab, F. J. Rixon, and D. Pasdeloup.** 2009. Differing Roles of Inner Tegument Proteins pUL36 and pUL37 During Entry of Herpes Simplex Virus Type 1 (HSV-1). J. Virol. **83:**105-116.
53. **Schipke, J., A. Pohlmann, R. Diestel, A. Binz, K. Rudolph, C. H. Nagel, R. Bauerfeind, and B. Sodeik.** 2012. The C terminus of the large tegument protein pUL36 contains multiple capsid binding sites that function differently during assembly and cell entry of herpes simplex virus. Journal of virology **86:**3682-3700.
54. **Schlieker, C., W. A. Weihofen, E. Frijns, L. M. Kattenhorn, R. Gaudet, and H. L. Ploegh.** 2007. Structure of a herpesvirus-encoded cysteine protease reveals a unique class of deubiquitinating enzymes. Mol. Cell. **25:**677-687.
55. **Shanda, S. K., and D. W. Wilson.** 2008. UL36p is required for efficient transport of membrane-associated herpes simplex virus type 1 along microtubules. Journal of virology **82:**7388-7394.
56. **Smith, G. A., and L. W. Enquist.** 2002. Break ins and break outs: viral interactions with the cytoskeleton of Mammalian cells. Annual review of cell and developmental biology **18:**135-161.
57. **Tischer, B. K., J. von Einem, B. Kaufer, and N. Osterrieder.** 2006. Two-step Red-mediated recombination for versatile high-efficiency markerless DNA manipulation in Escherichia coli. Biotechniques **40:**191-197.
58. **Trotman, L. C., N. Mosberger, M. Fornerod, R. P. Stidwill, and U. F. Greber.** 2001. Import of adenovirus DNA involves the nuclear pore complex receptor CAN/Nup214 and histone H1. Nature cell biology **3:**1092-1100.
59. **Vittone, V., E. Diefenbach, D. Triffett, M. W. Douglas, A. L. Cunningham, and R. J. Diefenbach.** 2005. Determination of interactions between tegument proteins of herpes simplex virus type 1. J. Virol. **79:**9566-9571.
60. **Whittaker, G. R., M. Kann, and A. Helenius.** 2000. Viral entry into the nucleus. Annual review of cell and developmental biology **16:**627-651.
61. **Wolfstein, A., C. H. Nagel, K. Radtke, K. Dohner, V. J. Allan, and B. Sodeik.** 2006. The inner tegument promotes herpes simplex virus capsid motility along microtubules in vitro. Traffic **7:**227-237.
62. **Zhou, L., E. Sokolskaja, C. Jolly, W. James, S. A. Cowley, and A. Fassati.** 2011. Transportin 3 promotes a nuclear maturation step required for efficient HIV-1 integration. PLoS pathogens **7:**e1002194.

1

2

3

FIGURE LEGENDS

Figure 1. Deletion of the VP1-2 abolishes plaque formation.

(a) Schematic summary of VP1-2, indicating the N-terminal USP domain, the highly basic NLS motif contained within a poorly conserved region, the large central region (grey) and a C-terminal conserved region (blue). Regions relevant to interactions with VP16, pUL37 and pUL25 are also indicated (10, 15, 30, 34, 41, 47, 59). (b) Serial dilutions of K.VP1-2ΔNLS were examined for plaque formation in complementing HS30 cells versus normal Vero cells. (c) Quantitative analysis of plaquing efficiency of the mutant versus KOS w/t in Vero and HS30 cells. Plaque formation is diminished by at least 7 logs and is essentially undetected in Vero cells compared to HS30 cells. (d) Comparison of the w/t and mutant strains in multi-step growth curve after low moi infection (0.01 pfu /cell, based on titres in complementing cells) in Vero (solid symbols) or HS30 (open symbols). Yields were titrated in HS30 cells. (e) Comparison of the w/t and mutant strain replication in single-step growth curves after high moi infection in Vero or HS30 (5 pfu /cell, based on titres in complementing cells).

Figure 2. Initial infection of single cells by K.VP1-2ΔNLS and failure to spread.

(a) Vero cells were infected with K.VP1-2ΔNLS or KOS w/t at a moi calculated to infect 1/500 cells. Monolayers were examined after three days for virus proteins by immunofluorescence. (ICP4, green; pUL37, red; nuclear counterstain blue). For the w/t virus, plaques had obviously grown and contained numerous antigen positive cells. In contrast for the mutant, single antigen positive cells were observed, (both antigens were detected though the red channel obscures the green in this merged example) but infection was never detected and did not progress in surrounding cells. (b) To examine the induction of expression of the w/t VP1-2 during propagation in complementing cells, RSC-HAUL36 cells were infected with K.VP1-2ΔNLS at a moi of 5 (based in titres in HS30 cells), samples harvested at the times indicated and examined for expression of the endogenous w/t VP1-2, by virtue of the HA-

tag, total VP1-2 using anti-VP1-2 or the major capsid protein VP5. Extracellular virus (see also Figure 5), from K.VP1-2ΔNLS and K.VP1-2ΔNLS.R amplified in the complementing RSC-HAUL36 cells, and purified by Ficoll gradient centrifugation were analysed to assess the incorporation of the endogenous VP1-2 into the virion particles produced in these cells in relation to VP5 (lanes 10,11).

Figure 3. Comparison of protein expression during infection by K.VP1-2ΔNLS and its revertant.

(a) RSC or RSC-HAUL36 cells were infected in parallel with the mutant K.VP1-2ΔNLS, the revertant K.VP1-2ΔNLS.R or KOS w/t virus at a moi of 5. Samples were harvested at the times indicated and expression of a series of delayed early or late proteins, VP5, pUL37, UL25, gD and VP1-2 itself was examined by Western blotting using fluorescent antibodies and quantitative detection as described in materials and methods. (b) As above, examining immediate-early (ICP4) or delayed early (ICP8) every h for 12 h. Some reduction was observed in the abundance of ICP4 (long arrow) though little significant difference for ICP8. (A non -specific band migrating just below ICP4 was occasionally observed, indicated by the short arrow). The parental KOS strain exhibited slightly increased expression of both proteins, estimated as 2-4 fold by quantitative analysis over the ΔNLS and ΔNLS.R viruses.

Figure 4. Comparison of protein localisation during infection by K.VP1-2ΔNLS and KOS w/t.

(a) Vero cells were infected with KOS or the mutant K.VP1-2ΔNLS virus at a moi of 5. Cultures were fixed after 16 h and processed for immunofluorescence as described. Patterns of localisation as discussed in the text were similar for both the w/t and mutant viruses. (b) RSC or Vero cells were infected and processed as in panel a and stained for VP1-2 localisation.

Figure 5. Ultrastructural analysis of capsid and virion formation in K.VP1-2ΔNLS infected cells.

RSC cells were infected in parallel with KOS or the mutant K.VP1-2ΔNLS at a moi of 5, fixed at 16 h post infection and processed for thin section electron microscopy as described in materials and methods. Sections for K.VP1-2ΔNLS are shown in panels a-c and for KOS in panel d-f. Capsid formation was readily apparent for both mutant and w/t viruses (panels a,d; small white arrows indicate nucleocapsids; large white arrowhead a particle in primary envelopment). Cytoplasmic envelopment was also observed for mutant and w/t viruses (panels b,e; black arrows indicate wrapping during secondary envelopment). Finally the presence of assembled virions are shown in example panels c and f for the mutant and revertant respectively. Panels g, and h show further examples of assembled extracellular virions readily observed for the mutant virus. Generally little difference in the main ultrastructural features of infection were observed for the w/t versus the mutant strains and all qualitative features of capsid and virion assembly could be observed. Similar results were obtained with K.VP1-2ΔNLS revertant virus and in different cell lines (Vero and HaCaT cells). Scale bars are 500 nm.

Figure 6. Characterisation of K.VP1-2ΔNLS^{NC} extracellular virus produced from non-complementing cells.

HaCaT cells were infected with K.VP1-2ΔNLS^{C} or the revertant virus at a moi of 5 (estimated from titration in complementing cells). We used HaCaT cells which we find helps increase overall yields of all herpesviruses strains. Media was harvested 16 h after infection, clarified and extracellular virus pelleted by centrifugation at 19k rpm for 90 min. Samples of pelleted virus showed slightly increased amounts of virion proteins for the mutant. Samples were adjusted (based on major capsid protein VP5) and analysed by SDS-PAGE. (a) Mutant and revertant virus exhibited similar qualitative and quantitative profiles of structural proteins including VP1-2, VP5. (b) Equalised samples were analysed by western blotting for the presence of a number of structural components as indicated. (c) Samples of extracellular particles from revertant or mutant infected cell medium, analysed by negative staining. Various

degrees of stain penetration were observed for both mutant and revertant and examples illustrating partially stained intact particles are shown for both. Scale bars are 200 nm. (d) Comparison of specific infectivity of K.VP1-2ΔNLS^{NC} and revertant extracellular virus particles, equalised on the basis of major capsid protein and titred for plaque formation in complementing HS30 cells. On a capsid standardised basis, K.VP1-2ΔNLS^{NC} particles exhibited approximately 600-fold lower infectivity. (e) Comparison of infectivity at the single cell level. Vero or HS30 cells were infected with serial dilutions of the revertant virus designed to give low moi infections within a range of 1:100 to 1:3 cells infected. Cells were infected in parallel with K.VP1-2ΔNLS^{NC} particles with an equivalent range based on equalised capsid protein. Cells were fixed 6 h after infection, stained with antibody to detect ICP4 and counterstained with DAPI to enumerate cells. Numerous cells were counted for each virus at each dilution. Typical fields shown are Vero cells with the highest amount of input virus to emphasis the difference in infectivity between the revertant and mutant, quantified in panel f. (g) Based on the titre of the revertant virus, cells were infected at high moi (5 pfu/cell) with the revertant virus or an equivalent input of mutant virus, based on standardisation of capsid protein in extracellular virus particles. Cells were harvested for Western blotting at the times indicated analysing in this case for a typical delayed-early protein ICP8, or the late major capsid protein VP5.

Figure 7. Immunofluorescence analysis of K.VP1-2ΔNLS^{NC} virus entry. Cells (RSC) were infected with extracellular virus of either the revertant ΔNLS.R or mutant virus ΔNLS produced from non-complementing cells. Infection was at a moi of 100 for the revertant or an equivalent amount of the mutant based on standardisation of VP5 in the extracellular purified virus. To help synchronise infection, cells were washed with cold media and incubated at 4°C after adding the inoculum. After 1 h, warmed media was added and the cells were further incubated for 2 or 4 h at 37°C prior to fixation and permeabilisation. Control samples maintained at 4°C were also examined as controls. Samples were stained for the major capsid protein VP5 and counterstained with DAPI to detect nuclei. The panels show typical examples

of many fields examined (using a x40 objective to capture multiple cells in each field), and present both channels for each virus at the indicated time. The VP5 channel only is shown in panels IV and VIII, highlighting the contrast between the revertant and mutant virus. Scale bars are 50 μm (b) High resolution confocal section of cells infected with the ΔNLS virus stained with anti-VP5 (green), anti-PCM1 (red) and DAPI (panel I; scale bar, 10 μm). The inset (scale bar, 2 μm) shows the pericentriolar PCM1 accumulations with congregating capsids in the same location, though the capsids do not necessarily directly overlap with the PCM1-specific material. Higher magnification images of capsids (VP5) and tegument proteins (pUL37 and VP1-2) colocalizing at the MTOC perinuclear accumulations of ΔNLS virus infection (panels II and III; scale bars are 5 μm) (c) Graph showing the quantification of the MTOC accumulation for revertant and mutant capsids. Defined and unbiased areas of interest were applied around the PCM1 pericentriolar region, and the accumulated density of pixels in the green channel for VP5 in the same areas calculated. Each vertical bar represents an individual cell. Approximately 130 cells were evaluated for each virus.

Figure 8. EM analysis showing nuclear pore interaction during entry of the ΔNLS revertant virus.

Vero cells were infected with the revertant virus K.VP1-2ΔNLS.R at an moi of 500 PFU/cell. The cells were washed with cold media and incubated at 4°C after adding the inoculum. After 1 h, warmed media was added and the cells incubated for 4 h at 37°C, then fixed and processed for thin section (70 nm) ultrastructural analysis as described in materials and methods. N and C indicate nucleus and cytoplasm respectively. An example section is shown with its inset illustrating the presence of empty capsids in close proximity to the nuclear pore. Additional insets are shown from additional independent sections illustrating the same feature of nuclear pore proximity and empty capsids. Scale bars are 500 nm in the main image and 250 nm for the insets. As is the case in thin section analysis, capsids immediately adjacent to the NE are only a subset of infecting capsids but were readily observed for the w/t

virus. Total numbers of capsids within 100 nm of the NE are quantitated in Figure 9c.

Figure 9. EM analysis of the block in K.VP1-2ΔNLS^{NC} virus entry.

In parallel with the analysis shown in Figure 8, cells were infected with the mutant virus K.VP1-2ΔNLS^{NC}, fixed and processed. N and C indicate nucleus and cytoplasm respectively. We readily detected cytoplasmic capsids, frequently in close proximity to the centrioles of the MTOC but capsids close to the NE were rare. (a) Representative field indicating the position within the cell and larger magnification in inset (b), showing full capsids of the infecting mutant. The single large arrowhead indicates the position of one of the centrioles with small arrows pointing to 6 capsids accumulated around the MTOC area. (c) Quantification of full and empty capsids from K.VP1-2ΔNLS and revertant infected cells. The total perimeter of the NE in 100 cells was scanned for capsids in close proximity (within 100 nm distance from the NE) and scored as empty or DNA-containing capsids. We found only rare examples of capsids close to the NE, these were not adjacent to pores and were DNA containing. Scale bars are 500nm.

Figure 10. Summary of propagation of K.VP1-2ΔNLS in complementing and normal cell types.

Three rows (a,b,c) summarise the outcomes of K.VP1-2ΔNLS infection. (a) Complementing cells (shaded in green) contain the w/t UL36 gene, which is induced after infection with K.VP1-2ΔNLS mutant (Figure 2b). The w/t VP1-2 is recruited onto virions (green virions with green dots indicating functional VP1-2 (Figure 2b). Note that a population of mutant VP1-2, indicated in orange could be recruited onto particles, and virions may have mixed populations and different distributions (a, II?). It may be that not all the VP1-2 incorporated needs to be w/t, though neither the distribution of w/t versus mutant VP1-2 nor the amount of w/t VP1-2 required for successful infection is known. The mutant can replicate, spread and form plaques in complementing cells. (b) Upon infection of non-complementing cells (shaded in grey) with the complemented virus, the virus can infect, undergo gene expression and

produce extracellular virus (orange virions) which now contains mutant VP1-2ΔNLS (orange dots, II). Our results indicate that this virus contains VP1-2ΔNLS and appears structurally similar to w/t virus with a similar cohort of proteins, can infect cells, but is blocked at the MTOC prior to successful nuclear engagement. (c) Producing K.VP1-2ΔNLS virus in non-complementing cells results in the formation of extracellular non-complemented virions. These virions have a profound block in infection at MTOC prior to nuclear engagement.

Figure 1

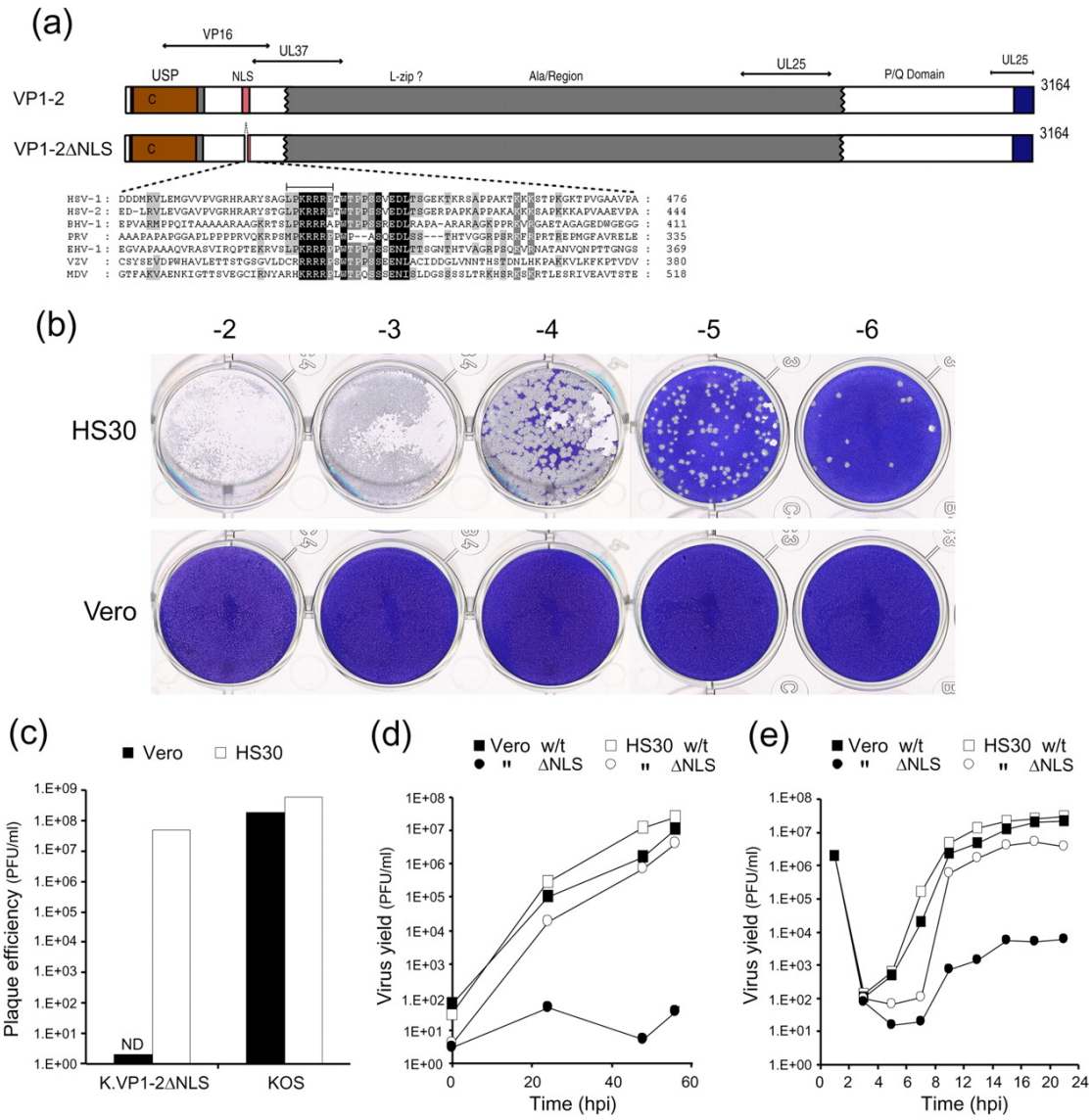
(a)
VP16
UL37
USP
NLS
L-zip ?
Ala/Region
UL25
P/Q Domain
UL25
VP1-2
VP1-2ΔNLS
3164
3164
HSV-1 : DDDMRVLEMGVVPVGRHRARYSAGLPKRRRETTTPPSSVEDLTSGEKTKRSAPPAKTGKSTPKGKTPVGAAVPA : 476
HSV-2 : ED-LRVLEVGAVPVGRHRARYSTGLPKRRRETTTPPSSVEDLTSGERPAPKAPPAKAGKSAPKKKAPVAAEVPA : 444
BHV-1 : EPVARMPPQITAAAAARAAGKRTSLPKRRRAPTTLPPSSREDLRAPA-ARARAGKPPRQVTGAETAGAGEDWGEGG : 411
PRV : AAAPAPAPGGAPLPPPPRVQKRPSMPKRRREPVP--ASGEDLSS---THTVGGRPSRPFPRTREPMGFAVRELE : 335
EHV-1 : EGVAPAAAQVRASVIRQPTEKRVSLPKRRRETTTPPSSENLTTSGNTHTVAGRPSQVTNATANVQNPTTGNGS : 369
VZV : CSYSEVDPWHAVLETTSTGSGVLDCRKRRRESTTPPSSENLACIDDGLVNNTHSTDNLHKPAKKVLKFKPTVDV : 380
MDV : GTFAKVAENKIGTTSVEGCIRNYARHKRRRELTTLQSSENISLDGSSSSLTRKHSRTSGRTLESRIVEAVTSTE : 518
(b)
-2
-3
-4
-5
-6
HS30
Vero
(c)
Vero
HS30
Plaque efficiency (PFU/ml)
1.E+09
1.E+08
1.E+07
1.E+06
1.E+05
1.E+04
1.E+03
1.E+02
1.E+01
1.E+00
ND
K.VP1-2ΔNLS
KOS
(d)
Vero w/t
HS30 w/t
" ΔNLS
" ΔNLS
Virus yield (PFU/ml)
1E+08
1E+07
1E+06
1E+05
1E+04
1E+03
1E+02
1E+01
1E+00
0
20
40
60
Time (hpi)
(e)
Vero w/t
HS30 w/t
" ΔNLS
" ΔNLS
Virus yield (PFU/ml)
1.E+08
1.E+07
1.E+06
1.E+05
1.E+04
1.E+03
1.E+02
1.E+01
1.E+00
0
2
4
6
8
12
14
16
20
24
Time (hpi)

Figure 2

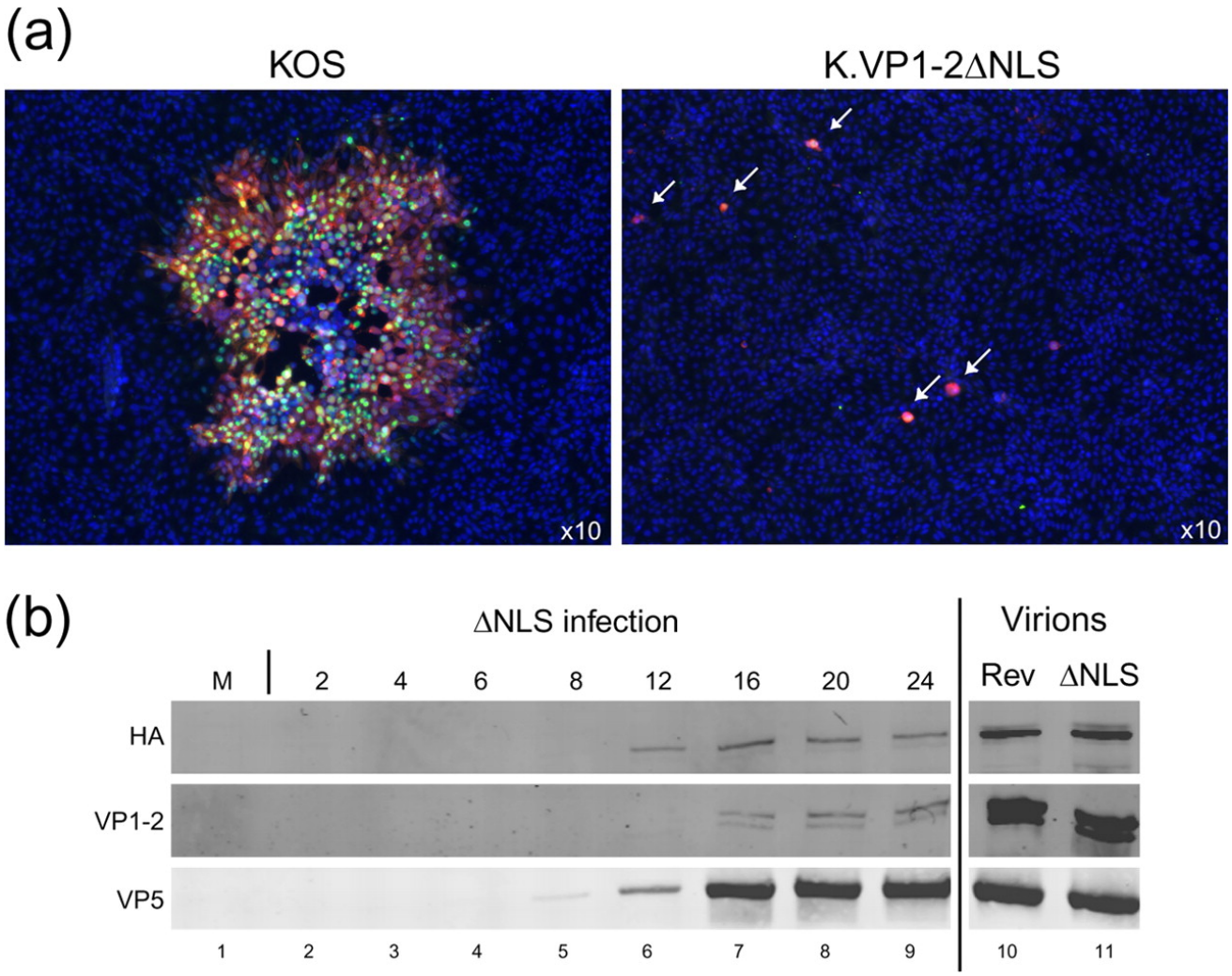
(a)
KOS
K.VP1-2ΔNLS
x10
x10
(b)
ΔNLS infection
Virions
M
2
4
6
8
12
16
20
24
Rev
ΔNLS
HA
VP1-2
VP5
1
2
3
4
5
6
7
8
9
10
11

Figure 3

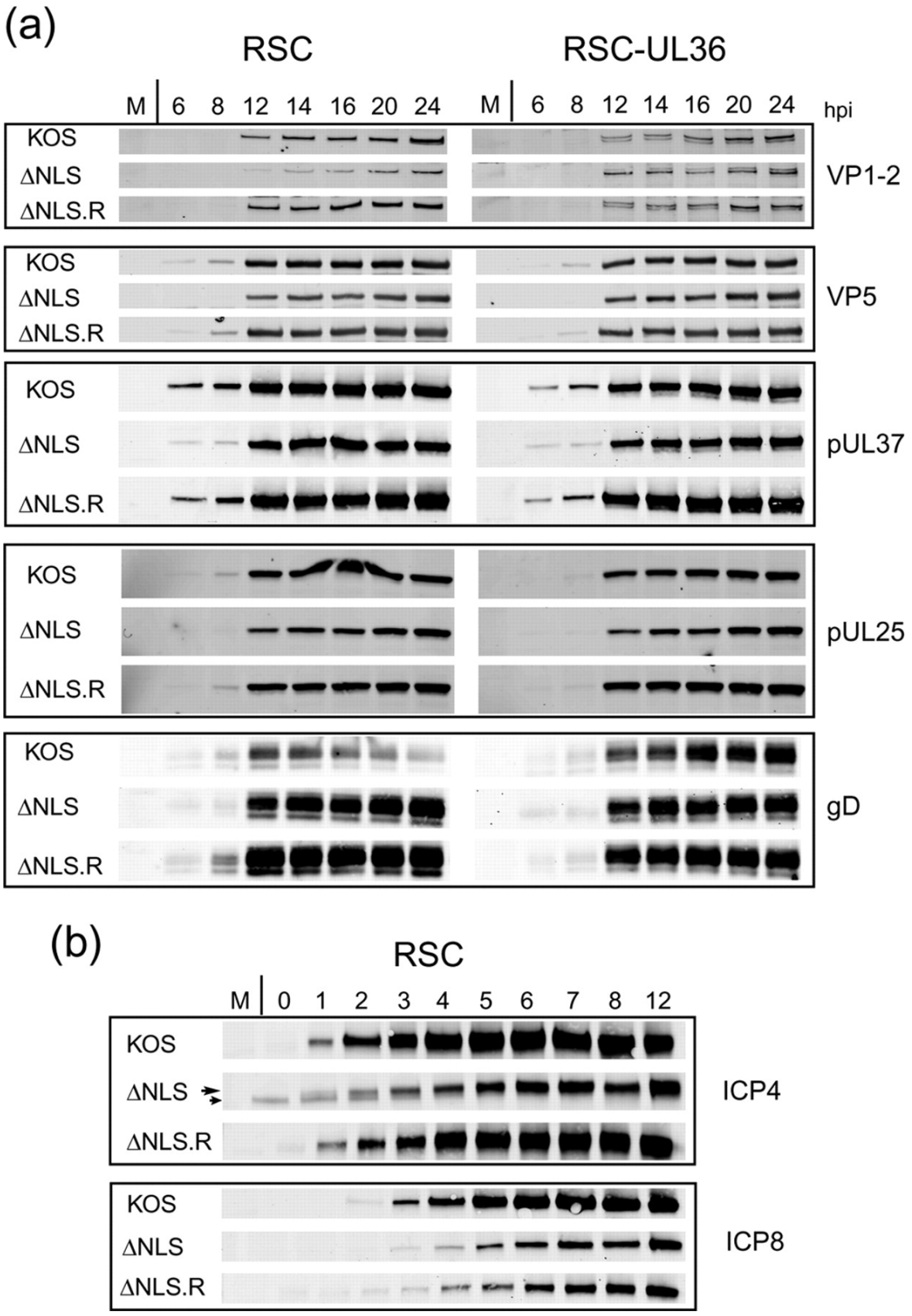
(a)
RSC
RSC-UL36
M 6 8 12 14 16 20 24 M 6 8 12 14 16 20 24 hpi
KOS
ΔNLS
ΔNLS.R
VP1-2
VP5
pUL37
pUL25
gD
(b)
RSC
M 0 1 2 3 4 5 6 7 8 12
ICP4
ICP8

Figure 4

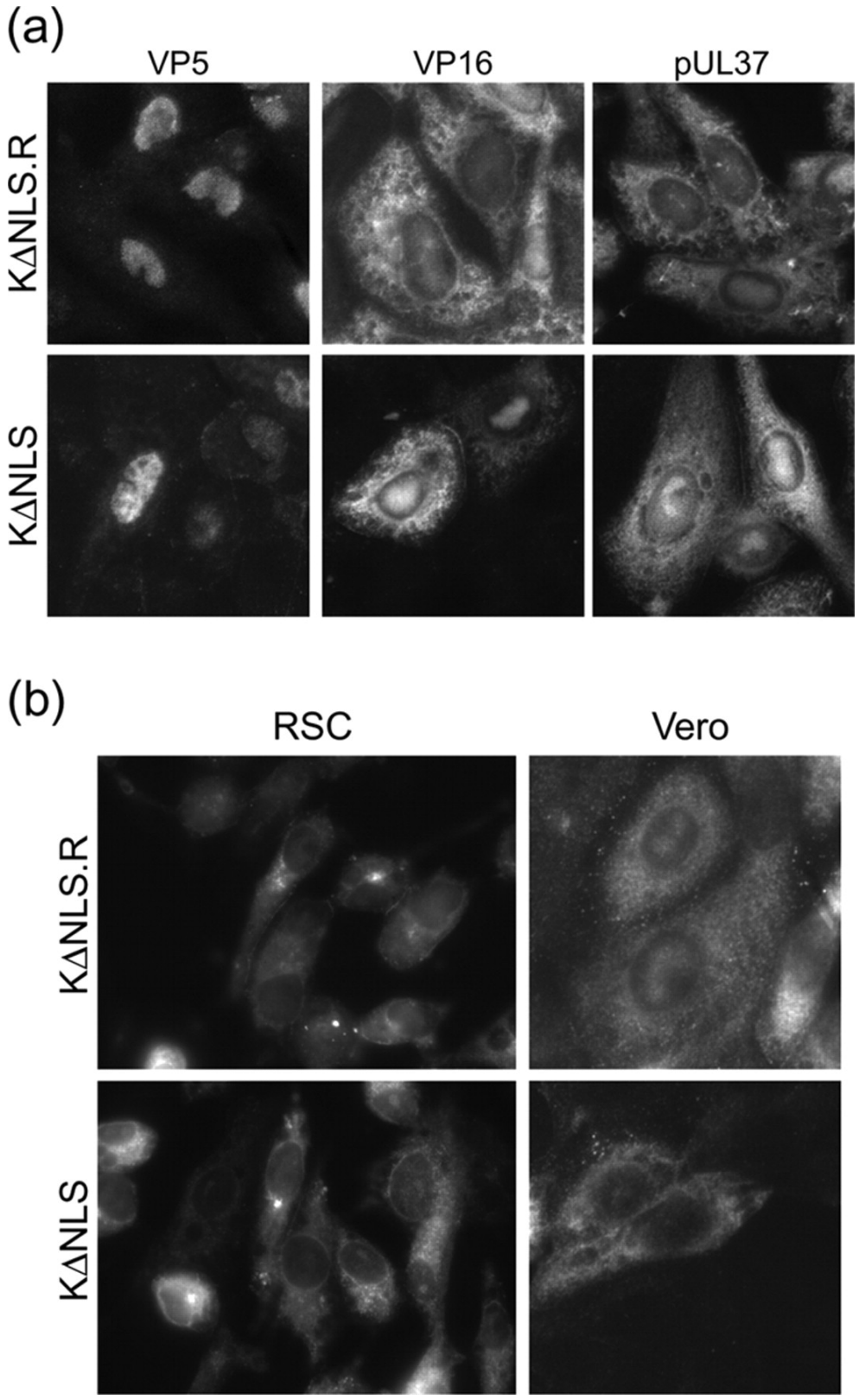

Figure 5

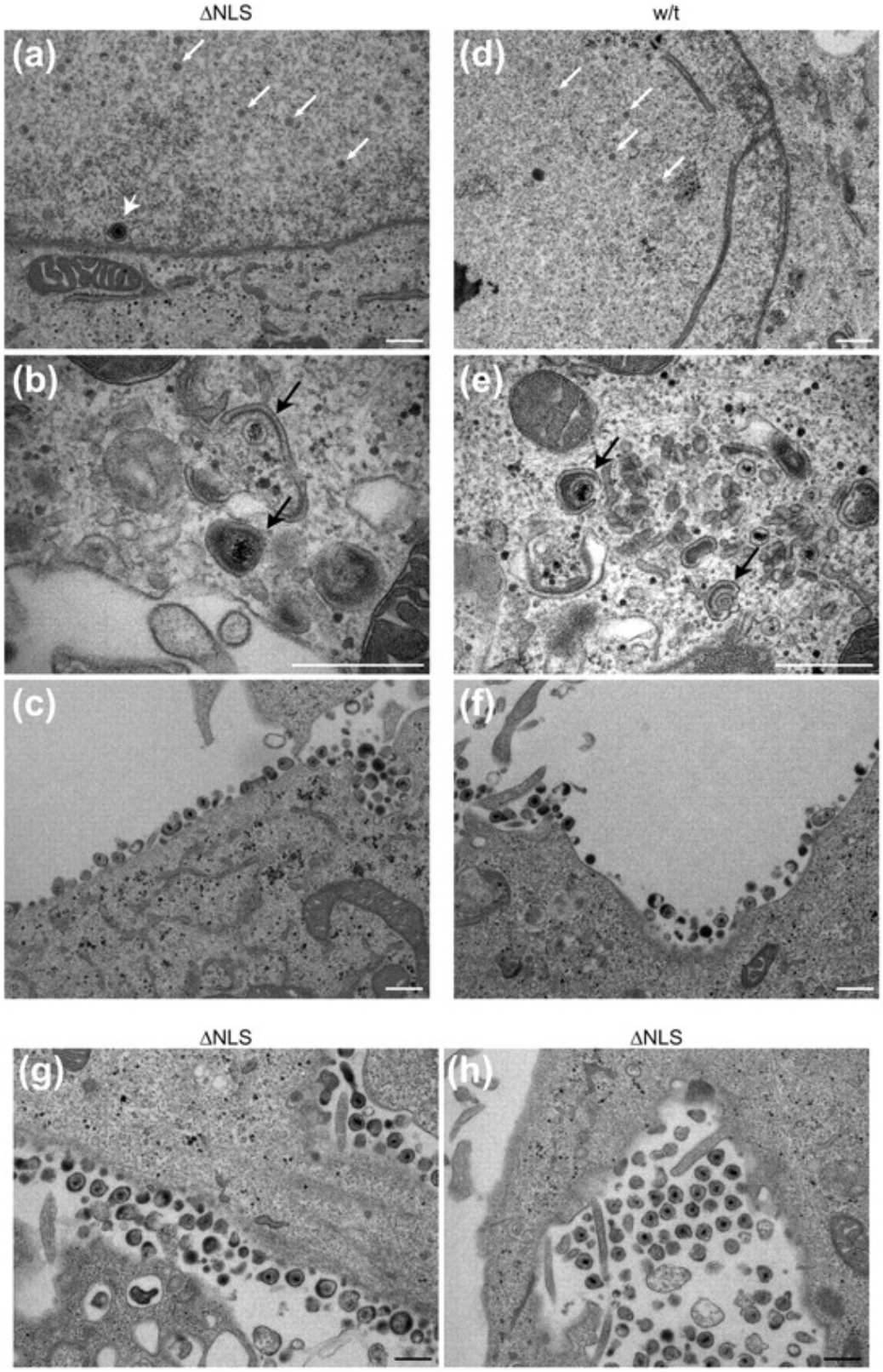

Figure 6

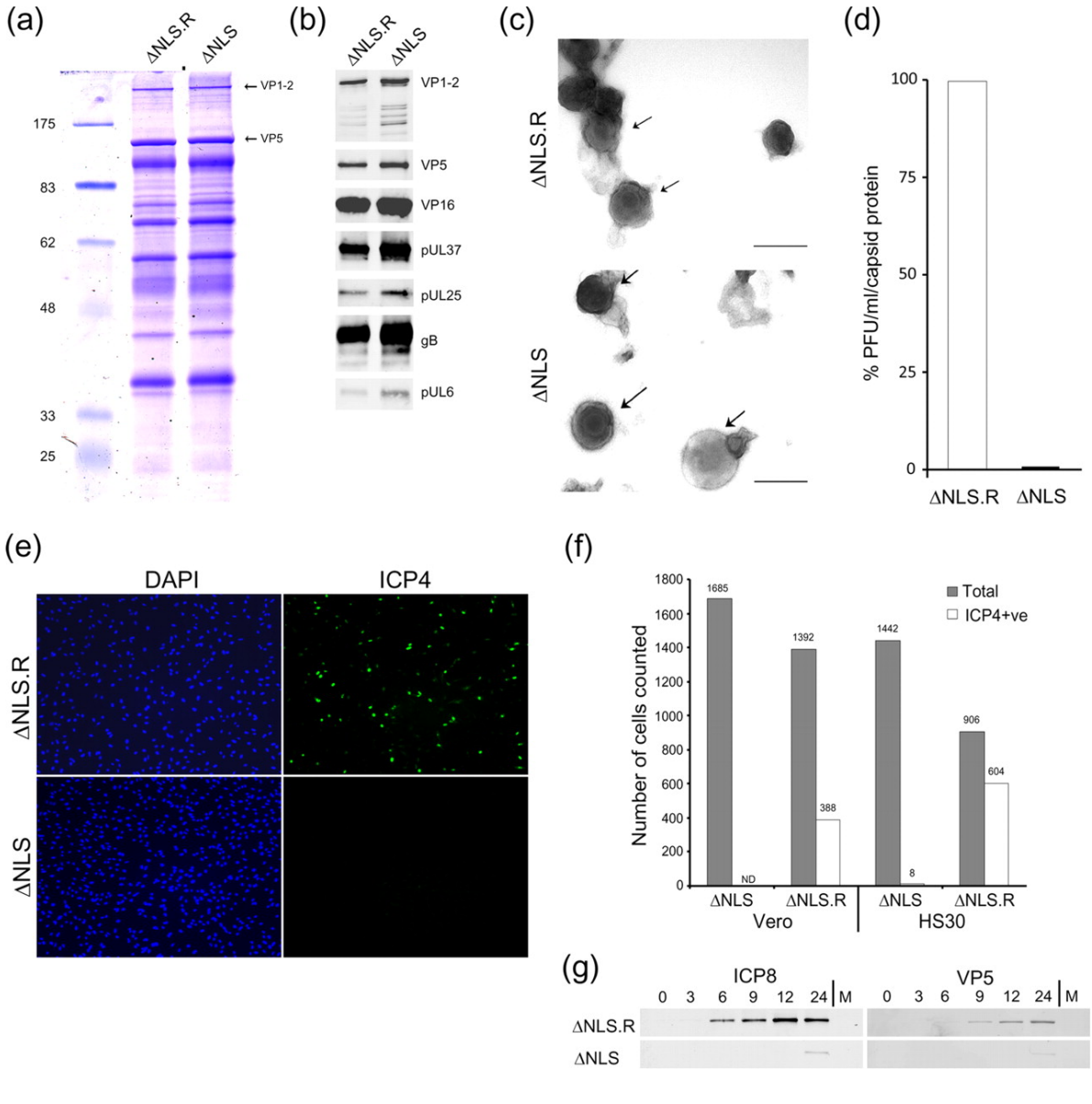
(a)
ΔNLS.R
ΔNLS
VP1-2
VP5
175
83
62
48
33
25
(b)
ΔNLS.R
ΔNLS
VP1-2
VP5
VP16
pUL37
pUL25
gB
pUL6
(c)
ΔNLS.R
ΔNLS
(d)
% PFU/ml/capsid protein
100
75
50
25
0
ΔNLS.R
ΔNLS
(e)
DAPI
ICP4
ΔNLS.R
ΔNLS
(f)
Number of cells counted
Total
ICP4+ve
1685
ND
1392
388
1442
8
906
604
ΔNLS
ΔNLS.R
ΔNLS
ΔNLS.R
Vero
HS30
(g)
ICP8
VP5
0 3 6 9 12 24 M
0 3 6 9 12 24 M
ΔNLS.R
ΔNLS

Figure 7

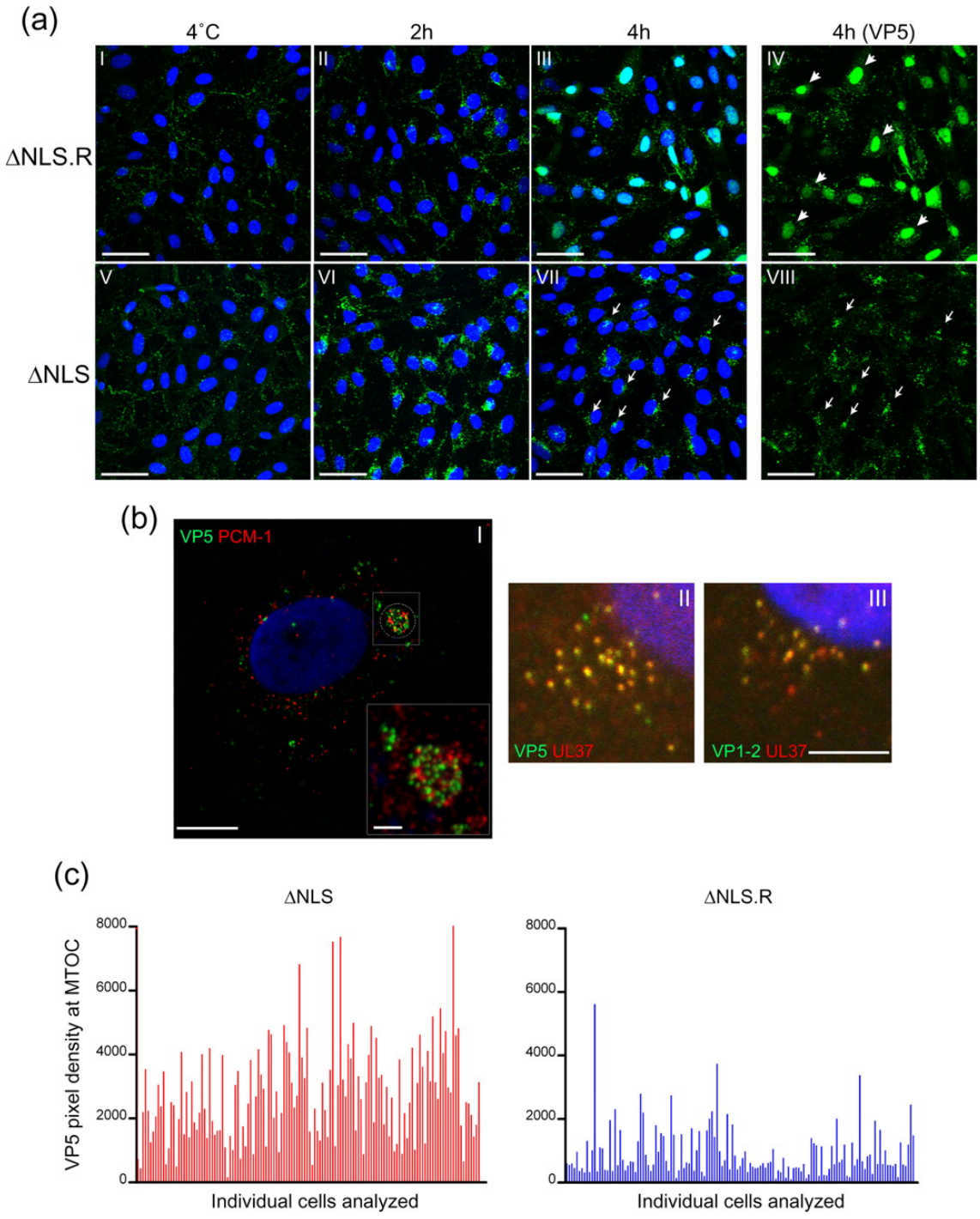
(a)
4˚C
2h
4h
4h (VP5)
I
II
III
IV
ΔNLS.R
V
VI
VII
VIII
ΔNLS
(b)
VP5 PCM-1
I
II
III
VP5 UL37
VP1-2 UL37
(c)
ΔNLS
ΔNLS.R
VP5 pixel density at MTOC
8000
6000
4000
2000
0
Individual cells analyzed

Figure 8

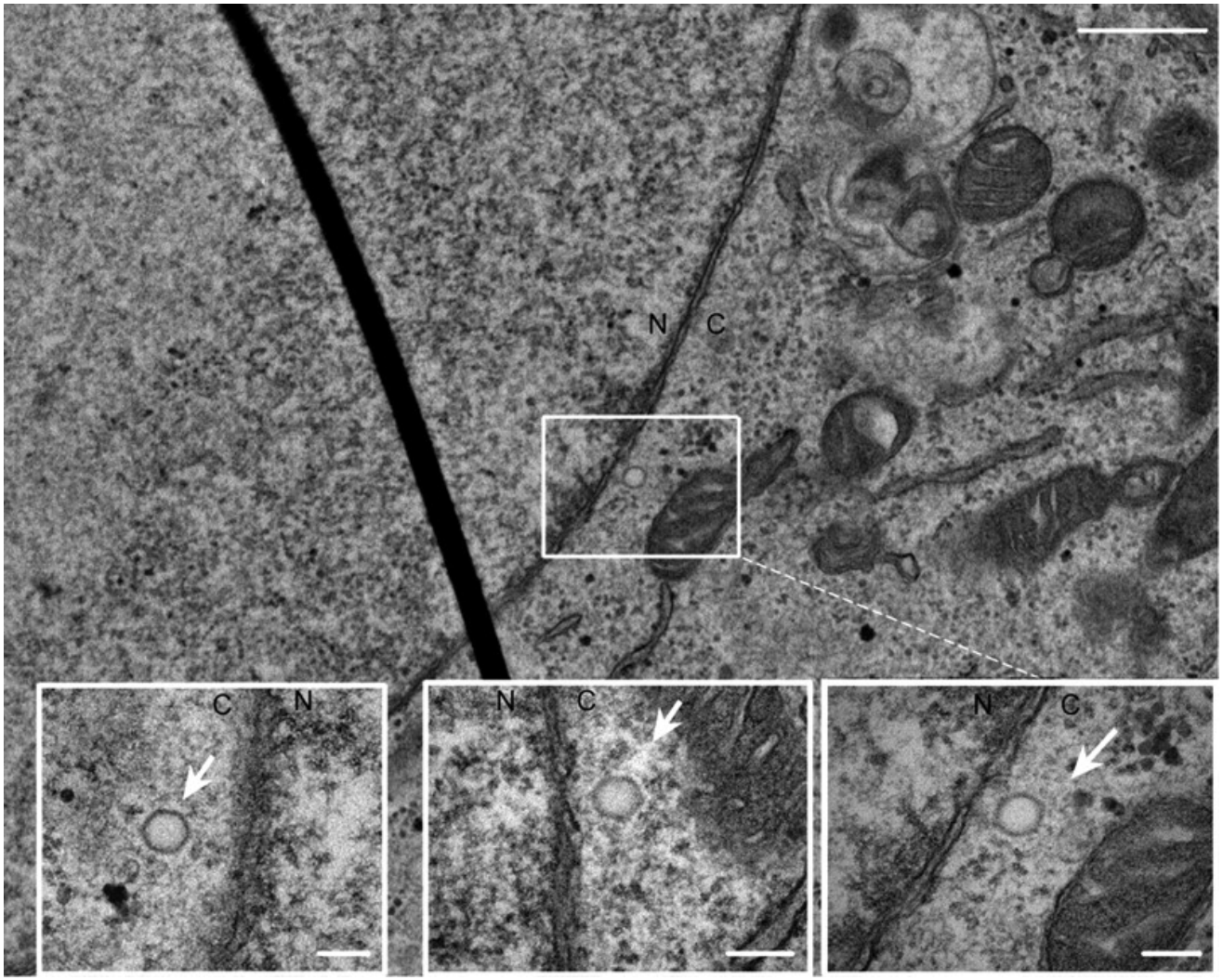

Figure 9

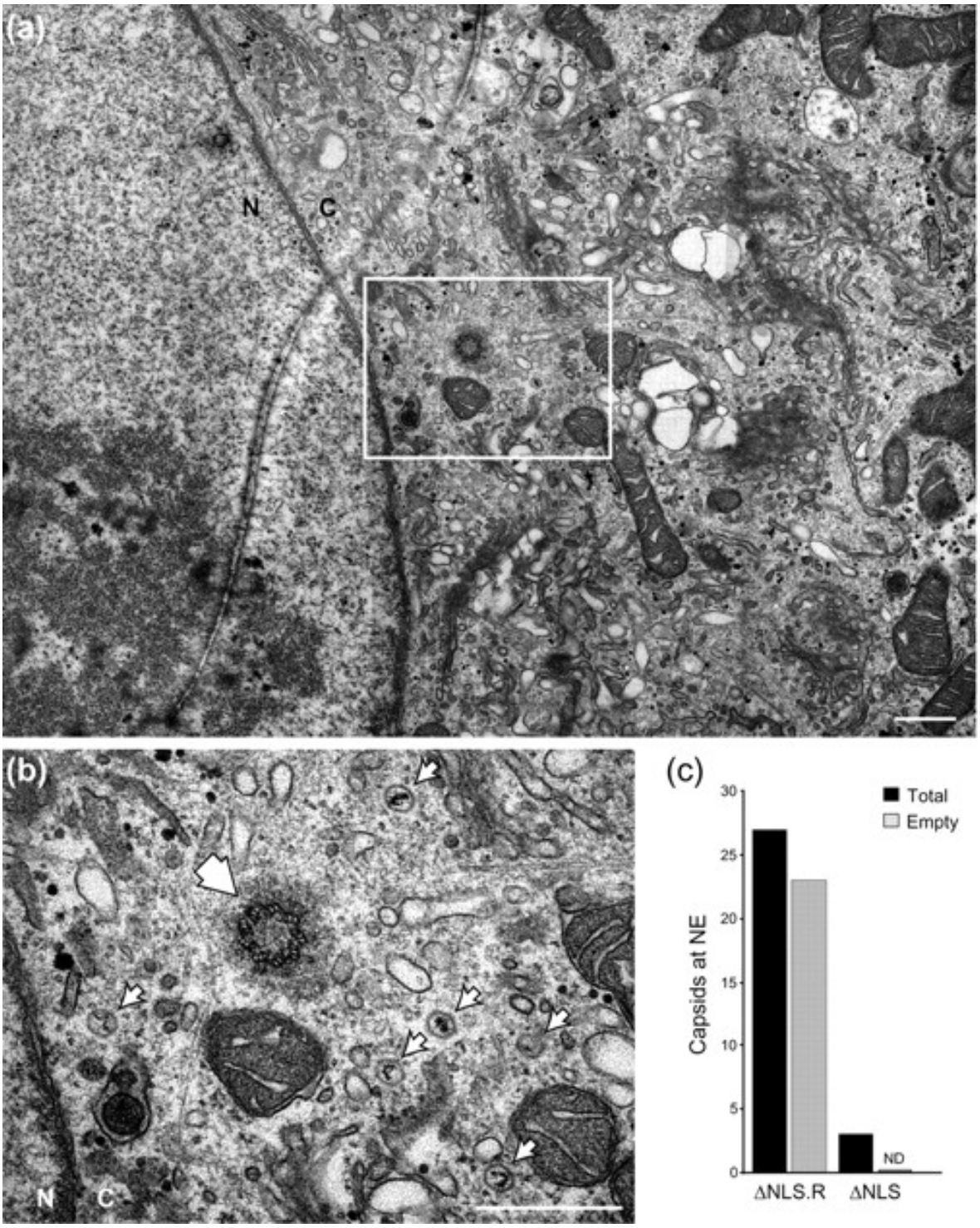
(a)
N
C
(b)
N
C
(c)
Total
Empty
Capsids at NE
30
25
20
15
10
5
0
ND
ΔNLS.R
ΔNLS

Figure 10

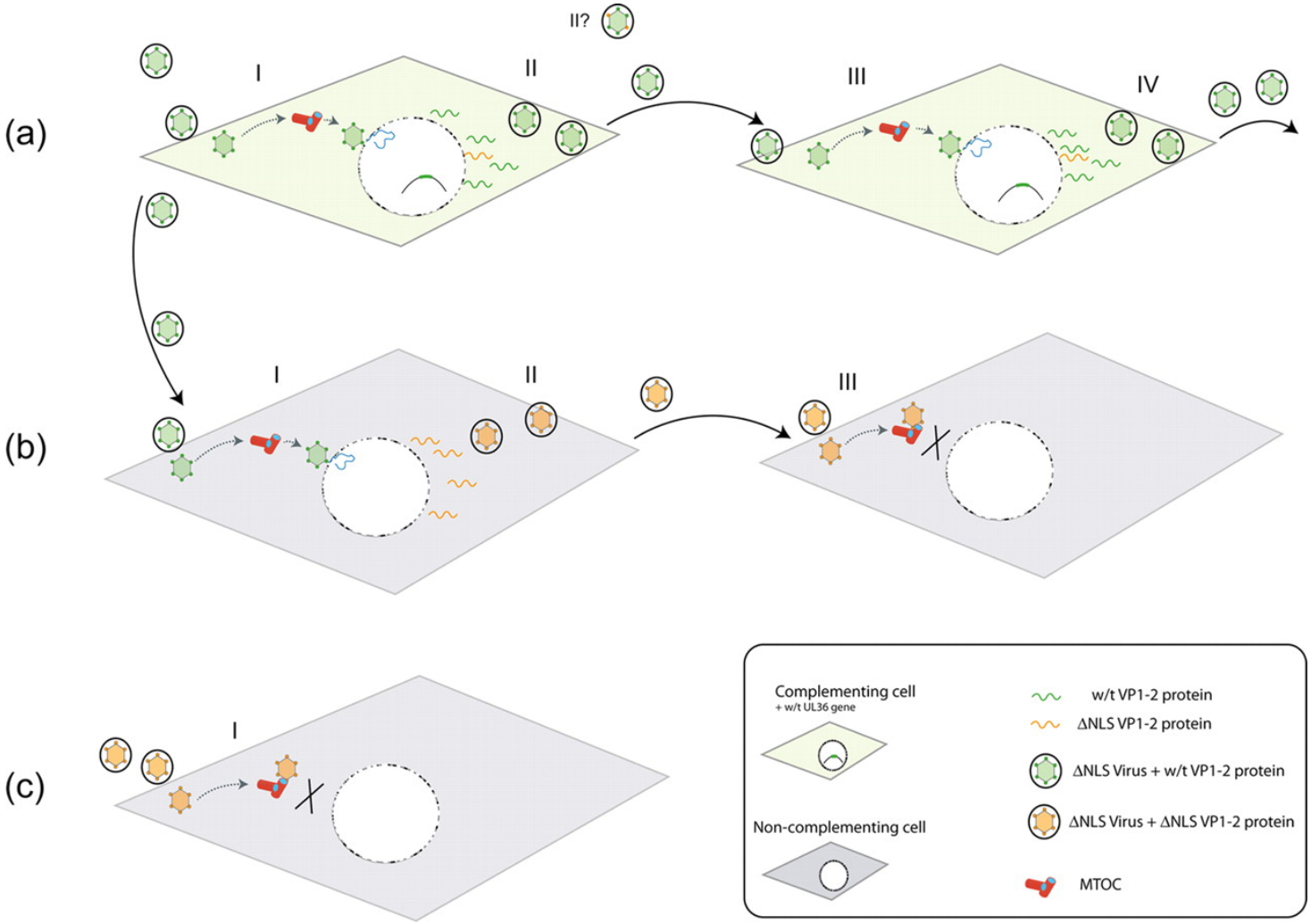
(a)
(b)
(c)
I
II
II?
III
IV
Complementing cell
+ w/t UL36 gene
Non-complementing cell
w/t VP1-2 protein
ΔNLS VP1-2 protein
ΔNLS Virus + w/t VP1-2 protein
ΔNLS Virus + ΔNLS VP1-2 protein
MTOC